Mathematical Biosciences and Engineering

http://www.aimspress.com/journal/mbe

MBE, 23(3): 636–677.
DOI: 10.3934/mbe.2026025
Received: 27 October 2025
Revised: 18 December 2025
Accepted: 04 January 2026
Published: 27 January 2026

Research article

Effects of multi-component small permanent charges on the dynamics of Poisson-Nernst-Planck models

Guojian Lin*

School of Mathematics, Renmin University of China, Beijing 100872, China

* **Correspondence:** Email: gjlin@ruc.edu.cn.

Abstract: In this paper, the classical Poisson-Nernst-Planck (PNP) model describing ion transport through a membrane channel is used to study the effects of small permanent charges and the structures of ion channels on ionic flows. The model under study includes two oppositely charged ion species, and the permanent charge in this model is a piecewise constant function with two nonzero regions. By rescaling, the classical PNP model can be viewed as a singularly perturbed differential equation system. Therefore, the geometric singular perturbation theory is employed to get a singular orbit. Assuming that the permanent charge density is small, a regular perturbation expansion is used to obtain the first-order approximation of the individual flux, which acts as a basis for our analysis. Then, the effects of small permanent charges on the fluxes and the current-voltage relation, which not only depend on the boundary conditions, but also depend on the structures of ion channels and the ratio between two nonzero permanent charge densities, are analyzed in this paper. Particularly, our results indicate that the geometric structures of three-dimensional ion channels have a short and narrow cross-section, which is explained in [1]. Also, our results indicate that the ratio between two nonzero permanent charge densities can change the position of a short and narrow cross-section in ion channels.

Keywords: PNP model; permanent charge; channel geometry; individual flux; I-V relation

1. Introduction

Ion channels are a class of proteins observed in cell membranes. These proteins form pores and accessory structures in the cell membrane, allowing specific ions to pass through while maintaining cellular homeostasis. They play important roles in cellular activity via controlling the flow of ions, and are fundamental elements in many basic biological processes from excitation and signaling to secretion and absorption. Therefore, ion channels are crucial to cell survival and function.

To understand the complex behavior of ion channels, molecular dynamics model is used, in which ion, water, and protein dynamics are described in atomic detail by making use of classical force

fields to describe molecular motions. To improve the computational efficiency in molecular dynamics simulations, Brownian dynamics and the Monte Carlo approach are developed; the former is based on the stochastic equation of the motions of ions, which describes some effective potential effects, and the latter computes the probability of the movement of a selected set of ion species by assuming that the ions are undergoing a random walk on a discrete mesh [2–6].

One of the most widely used models to describe ionic transport and electrostatic interactions in ion channels is the Poisson-Nernst-Planck (PNP) model which couples the Poisson equation for the electric potential with the Nernst–Planck equations that describe the fluxes of ionic species under the influence of both electrical and concentration gradients [7–15]. As a mean field continuum theory, the ion species involved in the PNP model are represented by macroscopic ion concentrations instead of microscopic discrete particles. Also, the PNP model can be derived from the Langevin-Poisson system [12, 16–20], the Maxwell-Boltzmann equations [5, 13, 18, 21], and the energy variational analysis [22–25]. Recently, researchers have employed coupled PNP and the Navier-Stokes equations to model ion channels, which provide a more detailed description of the ionic distribution [22, 26–29].

In this paper, the following one-dimensional version of the steady-state PNP type model [30, 31] is studied:

$$\begin{aligned} &\frac{1}{h(x)}\frac{d}{dx}\left(\varepsilon_r(x)\varepsilon_0 h(x)\frac{d\Phi}{dx}\right) = -e\left(\sum_{j=1}^{n} z_j c_j(x) + Q(x)\right), \\ &\frac{d\mathcal{J}_i}{dx} = 0, \quad -\mathcal{J}_i = \frac{1}{k_B T} D_i(x) h(x) c_i(x)\frac{d\mu_i}{dx}, \quad i = 1, 2, \cdots, n, \end{aligned} \tag{1.1}$$

where $x \in [0, 1]$ is the coordinate along the axis of the channel that is normalized to $[0, 1]$, e is the elementary charge, k_B the Boltzmann constant, T the absolute temperature, Φ is the electric potential, $Q(x)$ is the permanent charge of the channel, $\varepsilon_r(x)$ is the relative dielectric coefficient, ε_0 is the vacuum permittivity, and $h(x)$ is the area of the cross-section of the channel over the point x. For the ith ion species, c_i is the concentration, z_i the valence (the number of charges per particle), μ_i the electrochemical potential, $\mathcal{J}_i$ the flux density, and $D_i(x)$ the diffusion coefficient. The boundary conditions are, for $i = 1, 2, \cdots, n$,

$$\Phi(0) = \mathcal{V}, \;\; c_i(0) = L_i > 0; \quad \Phi(1) = 0, \;\; c_i(1) = R_i > 0. \tag{1.2}$$

An important characteristic for ion channels is the *I-V (current-voltage)* relation. Given a solution of the boundary value problem (1.1) and (1.2), the *current* $\mathcal{I}$ is

$$\mathcal{I} = \sum_{i=1}^{n} z_i \mathcal{J}_i. \tag{1.3}$$

If boundary concentrations L_i's and R_i's are fixed, then $\mathcal{J}_i$'s depend on $\mathcal{V}$ only and Eq (1.3) provides a dependence of the current $\mathcal{I}$ on the voltage $\mathcal{V}$.

The electrochemical potential $\mu_i(x)$ in (1.1) for the ith ion is decomposed into the ideal component $\mu_i^{id}(x)$ and the excess component $\mu_i^{ex}(x)$, where

$$\mu_i^{id}(x) = z_i e\phi(x) + k_B T \ln \frac{c_i(x)}{c_0} \tag{1.4}$$

with some characteristic number density c_0.

The classical PNP model only includes the ideal component $\mu_i^{id}(x)$ but does not take the excess component $\mu_i^{ex}(x)$ into consideration, which means that ions are treated as volumeless point charges, and water molecules are also treated as a dielectric medium without volumes. In the classical PNP model, the ideal component $\mu_i^{id}(x)$ reflects the collision between ion particles and the water molecules, but ion-ion and ion-water interactions are ignored. There are a great deal of works related to study the classical PNP model by numerical simulations [2,7,11,12,18,31–34] and theoretical analysis [1,35–50].

When ions are crowded in a highly narrow ion channel, the ion size effects must be included in describing ion transport. The excess component $\mu_i^{ex}(x)$ accounts for ion sizes, which are also relevant to the selectivity of ion channels. To include ion size effects, some modifications have been developed to improve the classical PNP model [24,51–53], and a lot of research has been done to understand the effects of ion sizes on the dynamics of the PNP model [12,22–25,52,54–58].

The classical PNP model incorporates the permanent charge description of ion channel proteins into the Poisson equation. In [1], the authors take the classical PNP model with two oppositely charged ion species to analyze the permanent charge effects on ionic flows under the assumption that the permanent charge $Q(x)$ is given by the following form:

$$Q(x) = \begin{cases} 0, & 0 < x < a, \\ Q_0, & a < x < b, \\ 0, & b < x < 1, \end{cases} \tag{1.5}$$

where Q_0 is a constant. For large $|Q_0|$, the existence of multiple solutions of the classical PNP model is justified in [37,40] by using the geometric singular perturbation theory [59,60]. However, explicit expressions for the fluxes are not available due to the computational complexity. For a small $|Q_0|$, let

$$\mathcal{J}_i = \mathcal{J}_{i0} + \mathcal{J}_{i1}Q_0 + O(Q_0^2),\ \mathcal{I} = \mathcal{I}_0 + \mathcal{I}_1 Q_0 + O(Q_0^2),\ i = 1,2, \tag{1.6}$$

and

$$H(x) = \int_0^x h^{-1}(s)ds,\ \alpha = \frac{H(a)}{H(1)},\ \beta = \frac{H(b)}{H(1)}. \tag{1.7}$$

Using a regular perturbation expansion, the authors in [1] obtain explicit expressions for the first-order approximation $\mathcal{J}_{i1}$, which is then used to show that small $|Q_0|$ strengthens or reduces the individual flux, and examine the signs of the first-order approximation $\mathcal{I}_1$ under some conditions. Furthermore, they analyze the maximum of $\mathcal{J}_{i1}$ with respect to the channel geometry (α,β) by fixing the boundary conditions, and the results in [1] support the structures of the ion channels.

The shape of a typical ion channel is often approximated as a cylindrical-like domain with variable cross-sectional areas along its axis. The spatial distribution of amino acid side chains within an ion channel defines the permanent charge of the channel, with acidic side chains contributing negative charges and basic side chains contributing positive charges. The ion channel shape and the permanent charge within an ion channel are closely related to the functions of an ion channel, such as selectivity, permeability and gating. As mentioned in [37,40], the permanent charge $Q(x)$ is reasonably modeled by a piecewise constant function with one nonzero region or multiple nonzero regions.

In this paper, it is assumed that the permanent charge $Q(x)$ takes the following form:

$$Q(x) = \begin{cases} 0, & 0 < x < a_1, \\ Q_1, & a_1 < x < b_1, \\ 0, & b_1 < x < a_2, \\ Q_2, & a_2 < x < b_2, \\ 0, & b_2 < x < 1, \end{cases} \tag{1.8}$$

where $|Q_1|$ and $|Q_2|$ are small relative to the boundary concentrations L_i's and R_i's. Obviously, letting $Q_1 = 0$ or $Q_2 = 0$, then (1.8) is reduced to (1.5).

Denote

$$\alpha_1 = \frac{H(a_1)}{H(1)},\ \beta_1 = \frac{H(b_1)}{H(1)},\ \alpha_2 = \frac{H(a_2)}{H(1)},\ \beta_2 = \frac{H(b_2)}{H(1)}. \tag{1.9}$$

The boundary value problem (1.1) and (1.2) is treated as a standard singularly perturbed problem in this paper. First, the geometric singular perturbation theory is employed to get a singular orbit solution for (1.1) and (1.2), then a regular perturbation expansion with respect to the small permanent charge is used to obtain explicit expressions for $\mathcal{J}_{i1}$. Finally, the effects of small permanent charges on the fluxes and the *I-V* relation, which not only depend on the boundary conditions, but also depend on the structures of ion channels $(\alpha_1, \beta_1, \alpha_2, \beta_2)$ and the ratio $\mu = \dfrac{Q_2}{Q_1}$, are analyzed. Particularly, our results indicate that the geometric structures of three-dimensional ion channels have a short and narrow cross-section, which is explained in [1]. Also, our results indicate that the ratio $\mu = \dfrac{Q_2}{Q_1}$ can change the position of a short and narrow cross-section in ion channels.

In comparison with the article [1], there are some difficult points to be solved.

1) Fixing the boundary conditions, $\mathcal{J}_{i1}$ only depends on two variables (α, β) in [1], but in this paper $\mathcal{J}_{i1}$ depends on four variables $(\alpha_1, \beta_1, \alpha_2, \beta_2)$ and the ratio $\mu = \dfrac{Q_2}{Q_1}$; it is this difference that gives rise to the difficulty for our analysis.

2) Lemma 4.6 in Section 4 in this paper is a new result which does not appear in [1], and it is crucial to analyze the effects of the permanent charge on the fluxes.

3) Fixing the boundary conditions, the maximum of the function $\mathcal{J}_{i1}$ in four variables $(\alpha_1, \beta_1, \alpha_2, \beta_2)$ in this paper is much more difficult to examine than that of the function $\mathcal{J}_{i1}$ in two variables (α, β) in [1].

The rest of the paper is organized as follows. In Section 2, the geometric singular perturbation framework for the classical PNP model is described, and a singular orbit of the boundary value problem of the PNP model is constructed. In Section 3, a regular perturbation expansion of a singular orbit with respect to small permanent charge is carried out, and extremely important formulae for $\mathcal{J}_{i1}$ are derived. In Section 4, the effects of the permanent charge on the fluxes, the maximum of $\mathcal{J}_{i1}$, and the signs of $\mathcal{I}_1$ are analyzed. Some conclusions are contained in Section 5. A proof of Proposition 3.4 is given in the Appendix.

2. Problem setup

For the boundary value problem (1.1) and (1.2), we make the following assumptions, which are basically the same as that in [1, 37]:

(A1). We consider two ion species ($n = 2$) with $z_1 > 0$ and $z_2 < 0$.
(A2). For the permanent charge $Q(x)$ in (1.8), we assume $|Q_1|$ and $|Q_2|$ are small relative to L_i's and R_i's.
(A3). For $\mu_i(x)$, we only include the ideal component $\mu_i^{id}(x)$, as in (1.4).
(A4). We assume that $\varepsilon_r(x) = \varepsilon_r$ and $D_i(x) = D_i$ are constants.

With rescaling, we get

$$\phi = \frac{e}{k_B T}\Phi, \quad V = \frac{e}{k_B T}\mathcal{V}, \quad \varepsilon^2 = \frac{\varepsilon_r \varepsilon_0 k_B T}{e^2}, \quad J_i = \frac{\mathcal{J}_i}{D_i},$$

and the expression (1.4) for $\mu_i(x)$=$\mu_i^{id}(x)$. The boundary value problem (1.1) and (1.2) becomes, for $i = 1, 2$,

$$\begin{aligned} &\frac{\varepsilon^2}{h(x)}\frac{d}{dx}\left(h(x)\frac{d}{dx}\phi\right) = -z_1 c_1 - z_2 c_2 + Q(x), \\ &h(x)\left(\frac{dc_i}{dx} + z_i c_i \frac{d\phi}{dx}\right) = -J_i, \ \frac{dJ_i}{dx} = 0, \end{aligned} \tag{2.1}$$

with the following boundary conditions:

$$\phi(0) = V, \quad c_i(0) = L_i; \quad \phi(1) = 0, \quad c_i(1) = R_i. \tag{2.2}$$

We will assume $\varepsilon > 0$ is small, and treat system (2.1) as a singularly perturbed system, and apply the geometric singular perturbation framework from [37, 40] for the boundary value problem (2.1) and (2.2).

Introduce $u = \varepsilon\dfrac{d}{dx}\phi$, $\tau = x$ and denote the derivative with respect to x by dot. System (2.1) becomes, for $i = 1, 2$,

$$\begin{aligned} &\varepsilon\dot{\phi} = u, \quad \varepsilon\dot{u} = -z_1 c_1 - z_2 c_2 - Q(\tau) - \varepsilon\frac{h_\tau(\tau)}{h(\tau)}u, \\ &\varepsilon\dot{c}_i = -z_i c_i u - \frac{\varepsilon}{h(\tau)}J_i, \ \dot{J}_i = 0, \quad \dot{\tau} = 1. \end{aligned} \tag{2.3}$$

System (2.3) will be treated as a dynamical system of phase space $\mathbb{R}^7$ with state variables $(\phi, u, c_1, c_2, J_1, J_2, \tau)$. System (2.3) is the so-called slow system. The rescaling $x = \varepsilon\xi$ of the independent variable x gives rise to the fast system, for $i = 1, 2$:

$$\begin{aligned} &\phi' = u, \quad u' = -z_1 c_1 - z_2 c_2 - Q(\tau) - \varepsilon\frac{h_\tau(\tau)}{h(\tau)}u, \\ &c_i' = -z_i c_i u - \frac{\varepsilon}{h(\tau)}J_i, \ J_i' = 0, \quad \tau' = \varepsilon, \end{aligned} \tag{2.4}$$

where prime denotes the derivative with respect to the variable ξ.

Let B_L and B_R be the subsets of the phase space $\mathbb{R}^7$ defined by

$$\begin{aligned} B_L =& \{(V, u, L_1, L_2, J_1, J_2, 0) \in \mathbb{R}^7 : \text{arbitrary } u, J_1, J_2\}, \\ B_R =& \{(0, u, R_1, R_2, J_1, J_2, 1) \in \mathbb{R}^7 : \text{arbitrary } u, J_1, J_2\}. \end{aligned} \tag{2.5}$$

Then, the original boundary value problem (2.1) and (2.2) is equivalent to a connecting problem, namely, finding a solution of (2.3) or (2.4) from B_L to B_R.

As developed in [37, 40], a common method to analyze this connecting problem of classical PNP models is first to reduce it to the limiting slow system by letting $\epsilon = 0$ in (2.3) and to the limiting fast system by letting $\epsilon = 0$ in (2.4), then a singular orbit for the connecting problem is constructed by matching slow orbits of the limiting slow system and fast orbits of the limiting fast system. Finally, exchange lemmas in [59, 60] can be used to show that there is a unique solution of the boundary value problem (2.1) and (2.2) for small $\varepsilon > 0$ in the vicinity of the singular orbit.

We now summarize the construction of a singular orbit derived in [37, 40].

Note that the permanent charge $Q(x)$ in (1.8) is discontinuous at $x = a_1, x = b_1, x = a_2$, and $x = b_2$. It is natural that the interval $[0, 1]$ is split into five subintervals: $[0, a_1]$, $[a_1, b_1]$, $[b_1, a_2]$, $[a_2, b_2]$, $[b_2, 1]$, and on each subinterval a singular orbit is constructed. Therefore, we preassign unknown values of ϕ, c_1 and c_2 at $x = a_1, x = b_1, x = a_2$, and $x = b_2$ as follows:

$$\begin{aligned}\phi(a_1) =&\phi^{a_1}, c_1(a_1) = c_1^{a_1}, c_2(a_1) = c_2^{a_1};\ \ \phi(b_1) = \phi^{b_1}, c_1(b_1) = c_1^{b_1}, c_2(b_1) = c_2^{b_1};\\ \phi(a_2) =&\phi^{a_2}, c_1(a_2) = c_1^{a_2}, c_2(a_2) = c_2^{a_2};\ \ \phi(b_2) = \phi^{b_2}, c_1(b_2) = c_1^{b_2}, c_2(b_2) = c_2^{b_2}.\end{aligned} \tag{2.6}$$

Let

$$\begin{aligned}B_{a_i} =&\{(\phi^{a_i}, u, c_1^{a_i}, c_2^{a_i}, J_1, J_2, a_i) \in \mathbb{R}^7 : \text{arbitrary } u, J_1, J_2\},\\ B_{b_i} =&\{(\phi^{b_i}, u, c_1^{b_i}, c_2^{b_i}, J_1, J_2, b_i) \in \mathbb{R}^7 : \text{arbitrary } u, J_1, J_2\}, i = 1, 2.\end{aligned}$$

Using these twelve unknowns, a singular orbit can be constructed on each subinterval from the following:

(i) The singular orbit on $[0, a_1]$ consists of two boundary layers (fast orbits) Γ^0 at $x = 0$, $\Gamma_l^{a_1}$ at $x = a_1$, and one regular layer (slow orbit) Λ_{0,a_1} over $(0, a_1)$, which connects from B_L to B_{a_1}. In particular, given $(\phi^{a_1}, c_1^{a_1}, c_2^{a_1})$, the scaled flux densities J_1^{0,a_1}, J_2^{0,a_1} over $(0, a_1)$ and the value $u_l(a_1)$ are uniquely determined.

(ii) The singular orbit on $[a_1, b_1]$ consists of two boundary layers (fast orbits) $\Gamma_r^{a_1}$ at $x = a_1$, $\Gamma_l^{b_1}$ at $x = b_1$ and one regular layer (slow orbit) Λ_{a_1,b_1} over (a_1, b_1), which connects from B_{a_1} to B_{b_1}. In particular, given $(\phi^{a_1}, c_1^{a_1}, c_2^{a_1})$ and $(\phi^{b_1}, c_1^{b_1}, c_2^{b_1})$, the scaled flux densities $J_1^{a_1,b_1}, J_2^{a_1,b_1}$ over (a_1, b_1) and the values $u_r(a_1)$ and $u_l(b_1)$ are uniquely determined.

(iii) The singular orbit on $[b_1, a_2]$ consists of two boundary layers (fast orbits) $\Gamma_r^{b_1}$ at $x = b_1$, $\Gamma_l^{a_2}$ at $x = a_2$ and one regular layer (slow orbit) Λ_{b_1,a_2} over (b_1, a_2), which connects from B_{b_1} to B_{a_2}. In particular, given $(\phi^{b_1}, c_1^{b_1}, c_2^{b_1})$ and $(\phi^{a_2}, c_1^{a_2}, c_2^{a_2})$, the scaled flux densities $J_1^{b_1,a_2}, J_2^{b_1,a_2}$ over (b_1, a_2) and the values $u_r(b_1)$ and $u_l(a_2)$ are uniquely determined.

(iv) The singular orbit on $[a_2, b_2]$ consists of two boundary layers (fast orbits) $\Gamma_r^{a_2}$ at $x = a_2$, $\Gamma_l^{b_2}$ at $x = b_2$ and one regular layer (slow orbit) Λ_{a_2,b_2} over (a_2, b_2), which connects from B_{a_2} to B_{b_2}. In particular, given $(\phi^{a_2}, c_1^{a_2}, c_2^{a_2})$ and $(\phi^{b_2}, c_1^{b_2}, c_2^{b_2})$, the scaled flux densities $J_1^{a_2,b_2}, J_2^{a_2,b_2}$ over (a_2, b_2) and the values $u_r(a_2)$ and $u_l(b_2)$ are uniquely determined.

(v) The singular orbit on $[b_2, 1]$ consists of two boundary layers (fast orbits) $\Gamma_r^{b_2}$ at $x = b_2$, Γ^1 at $x = 1$ and one regular layer (slow orbit) $\Lambda_{b_2,1}$ over $(b_2, 1)$, which connects from B_{b_2} to B_R. In particular, given $(\phi^{b_2}, c_1^{b_2}, c_2^{b_2})$, the scaled flux densities $J_1^{b_2,1}, J_2^{b_2,1}$ over $(b_2, 1)$ and the value $u_r(b_2)$ are uniquely determined.

To obtain a singular orbit on $[0,1]$, one requires the following matching conditions:

$$\begin{aligned} J_1^{0,a_1} =& J_1^{a_1,b_1} = J_1^{b_1,a_2} = J_1^{a_2,b_2} = J_1^{b_2,1};\\ J_2^{0,a_1} =& J_2^{a_1,b_1} = J_2^{b_1,a_2} = J_2^{a_2,b_2} = J_2^{b_2,1};\\ u_l(a_1) =& u_r(a_1),\ u_l(b_1) = u_r(b_1),\ u_l(a_2) = u_r(a_2),\ u_l(b_2) = u_r(b_2). \end{aligned} \tag{2.7}$$

Note that the number of twelve conditions in (2.7) is exactly equal to that of twelve unknowns preassigned in (2.6). Just as shown in [1, 37], the matching conditions in (2.7) can reduce the singular connecting problem to the system (43) in [37], which can be recast below for $i = 1, 2$:

$$\begin{aligned} &z_1 c_1^{a_i} e^{z_1(\phi^{a_i}-\phi^{a_i,r})} + z_2 c_2^{a_i} e^{z_2(\phi^{a_i}-\phi^{a_i,r})} + Q_i = 0,\\ &z_1 c_1^{b_i} e^{z_1(\phi^{b_i}-\phi^{b_i,l})} + z_2 c_2^{b_i} e^{z_2(\phi^{b_i}-\phi^{b_i,l})} + Q_i = 0,\\ &\frac{z_2-z_1}{z_2} c_1^{a_i,l} = c_1^{a_i} e^{z_1(\phi^{a_i}-\phi^{a_i,r})} + c_2^{a_i} e^{z_2(\phi^{a_i}-\phi^{a_i,r})} + Q_i(\phi^{a_i}-\phi^{a_i,r}),\\ &\frac{z_2-z_1}{z_2} c_1^{b_i,r} = c_1^{b_i} e^{z_1(\phi^{b_i}-\phi^{b_i,l})} + c_2^{b_i} e^{z_2(\phi^{b_i}-\phi^{b_i,l})} + Q_i(\phi^{b_i}-\phi^{b_i,l}),\\ &J_1 = \frac{c_1^L - c_1^{a_1,l}}{H(a_1)}\Big[1 + \frac{z_1(\phi^L-\phi^{a_1,l})}{\ln c_1^L - \ln c_1^{a_1,l}}\Big] = \frac{c_1^{b_2,r} - c_1^R}{H(1)-H(b_2)}\Big[1 + \frac{z_1(\phi^{b_2,r}-\phi^R)}{\ln c_1^{b_2,r} - \ln c_1^R}\Big]\\ &\quad = \frac{c_1^{b_1,r} - c_1^{a_2,l}}{H(a_2)-H(b_1)}\Big[1 + \frac{z_1(\phi^{b_1,r}-\phi^{a_2,l})}{\ln c_1^{b_1,r} - \ln c_1^{a_2,l}}\Big],\\ &J_2 = \frac{c_2^L - c_2^{a_1,l}}{H(a_1)}\Big[1 + \frac{z_2(\phi^L-\phi^{a_1,l})}{\ln c_2^L - \ln c_2^{a_1,l}}\Big] = \frac{c_2^{b_2,r} - c_2^R}{H(1)-H(b_2)}\Big[1 + \frac{z_2(\phi^{b_2,r}-\phi^R)}{\ln c_2^{b_2,r} - \ln c_2^R}\Big]\\ &\quad = \frac{c_2^{b_1,r} - c_2^{a_2,l}}{H(a_2)-H(b_1)}\Big[1 + \frac{z_2(\phi^{b_1,r}-\phi^{a_2,l})}{\ln c_2^{b_1,r} - \ln c_2^{a_2,l}}\Big],\\ &\phi^{b_i,l} = \phi^{a_i,r} - (z_1 J_1 + z_2 J_2) y_i,\\ &c_1^{b_i,l} = e^{z_1 z_2 (J_1+J_2) y_i} c_1^{a_i,r} - \frac{Q_i J_1}{z_1(J_1+J_2)}\Big[1 - e^{z_1 z_2 (J_1+J_2) y_i}\Big],\\ &J_1 + J_2 = -\frac{(z_1-z_2)(c_1^{a_i,r} - c_1^{b_i,l}) + z_2 Q_i(\phi^{a_i,r}-\phi^{b_i,l})}{z_2[H(b_i)-H(a_i)]}, \end{aligned} \tag{2.8}$$

where $y_i > 0$ are also unknowns, and related symbols are collected in Table 1.

Remark 2.1. *The symbol $\phi^{a_i,r}$ denotes the unique solution for the first equality in (2.8), which dose not have an explicit formula. Similarly, the symbol $\phi^{b_i,l}$ denotes the unique solution for the second equality in (2.8), which does not have an explicit formula.*

It can be seen that a solution for (2.8) can determine a singular orbit $(\Gamma^0 \cup \Lambda_{0,a_1} \cup \Gamma_l^{a_1}) \cup (\Gamma_r^{a_1} \cup \Lambda_{a_1,b_1} \cup \Gamma_l^{b_1}) \cup (\Gamma_r^{b_1} \cup \Lambda_{b_1,a_2} \cup \Gamma_l^{a_2}) \cup (\Gamma_r^{a_2} \cup \Lambda_{a_2,b_2} \cup \Gamma_l^{b_2}) \cup (\Gamma_r^{b_2} \cup \Lambda_{b_2,1} \cup \Gamma^1)$, which connects B_L and B_R; see Figure 1 for an illustration.

Table 1. Symbols.

Column 1	Column 2
$\phi^L = V - \frac{1}{z_1-z_2}\ln\frac{-z_2L_2}{z_1L_1}$	$\phi^R = -\frac{1}{z_1-z_2}\ln\frac{-z_2R_2}{z_1R_1}$
$c_1^L = \frac{1}{z_1}(z_1L_1)^{\frac{-z_2}{z_1-z_2}}(-z_2L_2)^{\frac{z_1}{z_1-z_2}}$	$c_2^L = -\frac{1}{z_2}(z_1L_1)^{\frac{-z_2}{z_1-z_2}}(-z_2L_2)^{\frac{z_1}{z_1-z_2}}$
$c_1^R = \frac{1}{z_1}(z_1R_1)^{\frac{-z_2}{z_1-z_2}}(-z_2R_2)^{\frac{z_1}{z_1-z_2}}$	$c_2^R = -\frac{1}{z_2}(z_1R_1)^{\frac{-z_2}{z_1-z_2}}(-z_2R_2)^{\frac{z_1}{z_1-z_2}}$
$\phi^{a_i,l} = \phi^{a_i} - \frac{1}{z_1-z_2}\ln\frac{-z_2c_2^{a_i}}{z_1c_1^{a_i}}$	$\phi^{b_i,r} = \phi^{b_i} - \frac{1}{z_1-z_2}\ln\frac{-z_2c_2^{b_i}}{z_1c_1^{b_i}}$
$c_1^{a_i,l} = \frac{1}{z_1}(z_1c_1^{a_i})^{\frac{-z_2}{z_1-z_2}}(-z_2c_2^{a_i})^{\frac{z_1}{z_1-z_2}}$	$c_2^{a_i,l} = -\frac{1}{z_2}(z_1c_1^{a_i})^{\frac{-z_2}{z_1-z_2}}(-z_2c_2^{a_i})^{\frac{z_1}{z_1-z_2}}$
$c_1^{b_i,r} = \frac{1}{z_1}(z_1c_1^{b_i})^{\frac{-z_2}{z_1-z_2}}(-z_2c_2^{b_i})^{\frac{z_1}{z_1-z_2}}$	$c_2^{b_i,r} = -\frac{1}{z_2}(z_1c_1^{b_i})^{\frac{-z_2}{z_1-z_2}}(-z_2c_2^{b_i})^{\frac{z_1}{z_1-z_2}}$
$c_1^{a_i,r} = e^{z_1(\phi^{a_i}-\phi^{a_i,r})}c_1^{a_i}$	$c_1^{b_i,l} = e^{z_1(\phi^{b_i}-\phi^{b_i,l})}c_1^{b_i}$

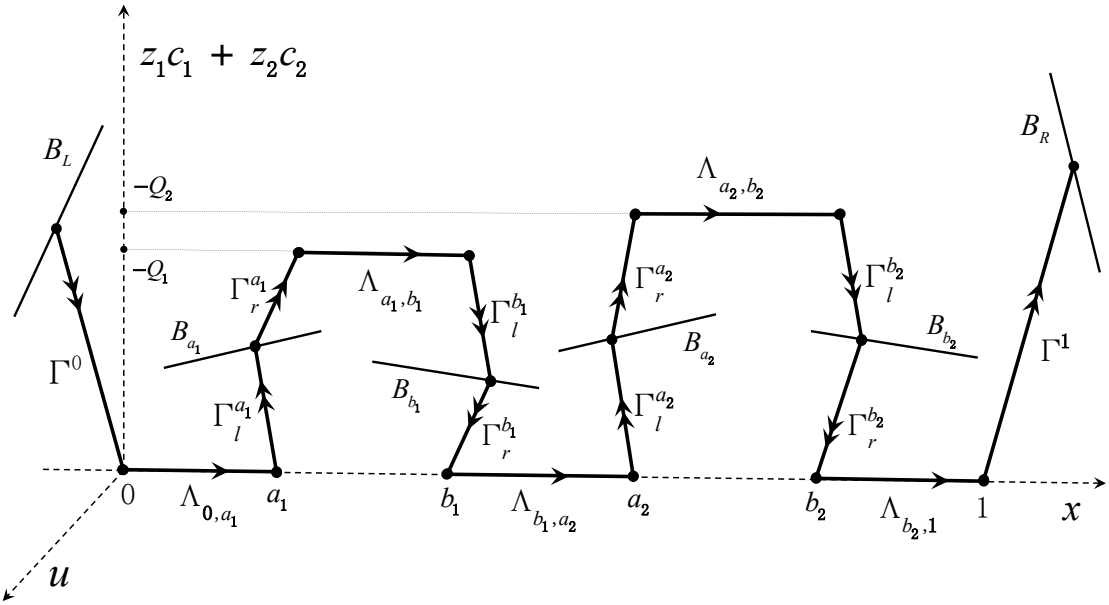

Figure 1. A singular orbit connecting B_L to B_R, where Γ^0, $\Gamma_l^{a_1}$, $\Gamma_r^{a_1}$, $\Gamma_l^{b_1}$, $\Gamma_r^{b_1}$, $\Gamma_l^{a_2}$, $\Gamma_r^{a_2}$, $\Gamma_l^{b_2}$, $\Gamma_r^{b_2}$, Γ^1 are limiting fast orbits and Λ_{0,a_1}, Λ_{a_1,b_1}, Λ_{b_1,a_2}, Λ_{a_2,b_2}, and $\Lambda_{b_2,1}$ are limiting slow orbits.

Moreover, once a singular orbit is constructed, then as shown in [37, 40], under some transversality conditions, it can verified that there is a unique solution of the boundary value problem (2.1) and (2.2) for small $\varepsilon > 0$ in the vicinity of the singular orbit by using exchange lemmas [59, 60].

In this paper, due to the assumption $(A2)$ that the constants $|Q_1|$ and $|Q_2|$ are small, then explicit expansions of a singular orbit with respect to Q_1 and Q_2 can be obtained in the next section.

For convenience, denote $Q_1 = Q$ and $Q_2 = \mu Q$, where the constant Q is small.

3. Expansion of singular solutions in small $|Q|$

In this section, it is assumed that the constant $|Q|$ is small. Therefore, we expand all unknown quantities in systems (2.8) in Q; namely, for $i = 1, 2$, let

$$\begin{aligned}
\phi^{a_i} &= \phi_0^{a_i} + \phi_1^{a_i} Q + \phi_2^{a_i} Q^2 + \cdots, & \phi^{b_i} &= \phi_0^{b_i} + \phi_1^{b_i} Q + \phi_2^{b_i} Q^2 + \cdots, \\
c_1^{a_i} &= c_{10}^{a_i} + c_{11}^{a_i} Q + c_{12}^{a_i} Q^2 + \cdots, & c_2^{a_i} &= c_{20}^{a_i} + c_{21}^{a_i} Q + c_{22}^{a_i} Q^2 + \cdots, \\
c_1^{b_i} &= c_{10}^{b_i} + c_{11}^{b_i} Q + c_{12}^{b_i} Q^2 + \cdots, & c_2^{b_i} &= c_{20}^{b_i} + c_{21}^{b_i} Q + c_{22}^{b_i} Q^2 + \cdots, \\
y_i &= y_{i0} + y_{i1} Q + y_{i2} Q^2 + \cdots, & J_i &= J_{i0} + J_{i1} Q + J_{i2} Q^2 + \cdots, \\
\phi^{a_i,r} &= \phi_0^{a_i,r} + \phi_1^{a_i,r} Q + \phi_2^{a_i,r} Q^2 + \cdots, & c_2^{a_i,l} &= c_{20}^{a_i,l} + c_{21}^{a_i,l} Q + c_{22}^{a_i,l} Q^2 + \cdots, \\
\phi^{a_i,l} &= \phi_0^{a_i,l} + \phi_1^{a_i,l} Q + \phi_2^{a_i,l} Q^2 + \cdots, & c_1^{b_i,l} &= c_{10}^{b_i,l} + c_{11}^{b_i,l} Q + c_{12}^{b_i,l} Q^2 + \cdots, \\
c_1^{a_i,l} &= c_{10}^{a_i,l} + c_{11}^{a_i,l} Q + c_{12}^{a_i,l} Q^2 + \cdots, & \phi^{b_i,l} &= \phi_0^{b_i,l} + \phi_1^{b_i,l} Q + \phi_2^{b_i,l} Q^2 + \cdots, \\
c_1^{b_i,r} &= c_{10}^{b_i,r} + c_{11}^{b_i,r} Q + c_{12}^{b_i,r} Q^2 + \cdots, & c_2^{b_i,r} &= c_{20}^{b_i,r} + c_{21}^{b_i,r} Q + c_{22}^{b_i,r} Q^2 + \cdots, \\
c_1^{a_i,r} &= c_{10}^{a_i,r} + c_{11}^{a_i,r} Q + c_{12}^{a_i,r} Q^2 + \cdots, & \phi^{b_i,r} &= \phi_0^{b_i,r} + \phi_1^{b_i,r} Q + \phi_2^{b_i,r} Q^2 + \cdots.
\end{aligned} \tag{3.1}$$

Then, by substituting (3.1) into (2.8), expanding the identities in Q, and comparing the terms of like-powers in Q, we can obtain the zeroth-order solution and the first-order solution of (2.8), which will be uesd to analyze effects of the permanent charge on ionic flows.

Remark 3.1. *For small Q and small $\epsilon > 0$, the existence of a unique solution for (2.8) is proved in [37, 40] in the vicinity of a singular orbit. For our purpose, unknown quantities in (3.1) are only expanded and calculated up to the first order.*

3.1. Zeroth-order solution in $|Q|$ of (2.8)

Actually, the zeroth-order solution of (2.8) has been solved in [37, 39]. We summarize the results below.

Proposition 3.2. *The zeroth-order solution in Q of (2.8) is given by, for $i = 1, 2$,*

$$c_{10}^{a_i} = c_1^L + \alpha_i (c_1^R - c_1^L),\ z_1 c_{10}^{a_i} = -z_2 c_{20}^{a_i},$$

$$c_{10}^{b_i} = c_1^L + \beta_i (c_1^R - c_1^L),\ z_1 c_{10}^{b_i} = -z_2 c_{20}^{b_i},$$

$$\phi_0^{a_i} = \frac{\ln c_1^R - \ln c_{10}^{a_i}}{\ln c_1^R - \ln c_1^L} \phi^L + \frac{\ln c_{10}^{a_i} - \ln c_1^L}{\ln c_1^R - \ln c_1^L} \phi^R,$$

$$\phi_0^{b_i} = \frac{\ln c_1^R - \ln c_{10}^{b_i}}{\ln c_1^R - \ln c_1^L}\phi^L + \frac{\ln c_{10}^{b_i} - \ln c_1^L}{\ln c_1^R - \ln c_1^L}\phi^R,$$

$$y_{i0} = \frac{H(1)}{z_1(z_1 - z_2)(c_1^R - c_1^L)} \ln \frac{(1-\beta_i)c_1^L + \beta_i c_1^R}{(1-\alpha_i)c_1^L + \alpha_i c_1^R},$$

$$J_{10} = \frac{c_1^L - c_1^R}{H(1)(\ln c_1^L - \ln c_1^R)}(z_1 V + \ln L_1 - \ln R_1),$$

$$J_{20} = \frac{c_2^L - c_2^R}{H(1)(\ln c_2^L - \ln c_2^R)}(z_2 V + \ln L_2 - \ln R_2).$$

Corollary 3.3. *Under electroneutrality boundary conditions $z_1L_1 = -z_2L_2 = L$ and $z_1R_1 = -z_2R_2 = R$, one has $c_1^L = L_1, c_2^L = L_2, c_1^R = R_1, c_2^R = R_2, \phi^L = V, \phi^R = 0$, and, for $i = 1, 2$,*

$$z_1 c_{10}^{a_i} = L + \alpha_i(R - L),\ z_1 c_{10}^{a_i} = -z_2 c_{20}^{a_i},$$

$$z_1 c_{10}^{b_i} = L + \beta_i(R - L),\ z_1 c_{10}^{b_i} = -z_2 c_{20}^{b_i},$$

$$\phi_0^{a_i} = \frac{\ln R - \ln[L + \alpha_i(R - L)]}{\ln R - \ln L} V,$$

$$\phi_0^{b_i} = \frac{\ln R - \ln[L + \beta_i(R - L)]}{\ln R - \ln L} V,$$

$$y_{i0} = \frac{H(1)}{(z_1 - z_2)(R - L)} \ln \frac{(1-\beta_i)L + \beta_i R}{(1-\alpha_i)L + \alpha_i R},$$

$$J_{10} = \frac{L - R}{z_1 H(1)(\ln L - \ln R)}(z_1 V + \ln L - \ln R),$$

$$J_{20} = -\frac{L - R}{z_2 H(1)(\ln L - \ln R)}(z_2 V + \ln L - \ln R).$$

3.2. First-order solution in $|Q|$ of (2.8)

Substituting (3.1) into (2.8), the first-order solution of (2.8) can be obtained by lengthy calculations.

Proposition 3.4. *First-order terms of the solution in Q of (2.8) are given by*

$$
\begin{aligned}
c_{11}^{a_1} &= \frac{z_2\alpha_1}{z_2-z_1}(\phi_0^{a_1}-\phi_0^{b_1})+\frac{z_2\alpha_1\mu}{z_2-z_1}(\phi_0^{a_2}-\phi_0^{b_2})+\frac{1}{2(z_2-z_1)},\\
c_{11}^{b_1} &= \frac{z_2(\beta_1-1)}{z_2-z_1}(\phi_0^{a_1}-\phi_0^{b_1})+\frac{z_2\beta_1\mu}{z_2-z_1}(\phi_0^{a_2}-\phi_0^{b_2})+\frac{1}{2(z_2-z_1)},\\
c_{11}^{a_2} &= \frac{z_2(\alpha_2-1)}{z_2-z_1}(\phi_0^{a_1}-\phi_0^{b_1})+\frac{z_2\alpha_2\mu}{z_2-z_1}(\phi_0^{a_2}-\phi_0^{b_2})+\frac{\mu}{2(z_2-z_1)},\\
c_{11}^{b_2} &= \frac{z_2(\beta_2-1)}{z_2-z_1}(\phi_0^{a_1}-\phi_0^{b_1})+\frac{z_2(\beta_2-1)\mu}{z_2-z_1}(\phi_0^{a_2}-\phi_0^{b_2})+\frac{\mu}{2(z_2-z_1)},\\
&z_1c_{11}^{a_1}+z_2c_{21}^{a_1}=-\frac{1}{2}, z_1c_{11}^{b_1}+z_2c_{21}^{b_1}=-\frac{1}{2},\\
&z_1c_{11}^{a_2}+z_2c_{21}^{a_2}=-\frac{\mu}{2}, z_1c_{11}^{b_2}+z_2c_{21}^{b_2}=-\frac{\mu}{2},\\
\phi_1^{a_1} &= \frac{(1+z_1\lambda)(1+z_2\lambda)(c_{10}^{a_1}-c_{10}^{b_1})(\ln c_1^L-\ln c_{10}^{a_1})}{z_1(z_1-z_2)c_{10}^{a_1}c_{10}^{b_1}(\ln c_1^L-\ln c_1^R)}\\
&\quad+\frac{(1+z_1\lambda)(1+z_2\lambda)(c_{10}^{a_2}-c_{10}^{b_2})(\ln c_1^L-\ln c_{10}^{a_1})\mu}{z_1(z_1-z_2)c_{10}^{a_2}c_{10}^{b_2}(\ln c_1^L-\ln c_1^R)}\\
&\quad+\frac{1}{2z_1(z_1-z_2)c_{10}^{a_1}}+\frac{\alpha_1(\phi_0^{b_1}-\phi_0^{a_1})z_2\lambda}{(z_1-z_2)c_{10}^{a_1}}+\frac{\alpha_1(\phi_0^{b_2}-\phi_0^{a_2})z_2\lambda\mu}{(z_1-z_2)c_{10}^{a_1}},\\
\phi_1^{b_1} &= \frac{(1+z_1\lambda)(1+z_2\lambda)(c_{10}^{a_1}-c_{10}^{b_1})(\ln c_1^R-\ln c_{10}^{b_1})}{z_1(z_1-z_2)c_{10}^{a_1}c_{10}^{b_1}(\ln c_1^L-\ln c_1^R)}\\
&\quad+\frac{(1+z_1\lambda)(1+z_2\lambda)(c_{10}^{a_2}-c_{10}^{b_2})(\ln c_1^L-\ln c_{10}^{b_1})\mu}{z_1(z_1-z_2)c_{10}^{a_2}c_{10}^{b_2}(\ln c_1^L-\ln c_1^R)}\\
&\quad+\frac{1}{2z_1(z_1-z_2)c_{10}^{b_1}}+\frac{(\beta_1-1)(\phi_0^{b_1}-\phi_0^{a_1})z_2\lambda}{(z_1-z_2)c_{10}^{b_1}}+\frac{\beta_1(\phi_0^{b_2}-\phi_0^{a_2})z_2\lambda\mu}{(z_1-z_2)c_{10}^{b_1}},\\
\phi_1^{a_2} &= \frac{(1+z_1\lambda)(1+z_2\lambda)(c_{10}^{a_1}-c_{10}^{b_1})(\ln c_1^R-\ln c_{10}^{a_2})}{z_1(z_1-z_2)c_{10}^{a_1}c_{10}^{b_1}(\ln c_1^L-\ln c_1^R)}\\
&\quad+\frac{(1+z_1\lambda)(1+z_2\lambda)(c_{10}^{a_2}-c_{10}^{b_2})(\ln c_1^L-\ln c_{10}^{a_2})\mu}{z_1(z_1-z_2)c_{10}^{a_2}c_{10}^{b_2}(\ln c_1^L-\ln c_1^R)}\\
&\quad+\frac{\mu}{2z_1(z_1-z_2)c_{10}^{a_2}}+\frac{(\alpha_2-1)(\phi_0^{b_1}-\phi_0^{a_1})z_2\lambda}{(z_1-z_2)c_{10}^{a_2}}+\frac{\alpha_2(\phi_0^{b_2}-\phi_0^{a_2})z_2\lambda\mu}{(z_1-z_2)c_{10}^{a_2}},\\
\phi_1^{b_2} &= \frac{(1+z_1\lambda)(1+z_2\lambda)(c_{10}^{a_1}-c_{10}^{b_1})(\ln c_1^R-\ln c_{10}^{b_2})}{z_1(z_1-z_2)c_{10}^{a_1}c_{10}^{b_1}(\ln c_1^L-\ln c_1^R)}\\
&\quad+\frac{(1+z_1\lambda)(1+z_2\lambda)(c_{10}^{a_2}-c_{10}^{b_2})(\ln c_1^R-\ln c_{10}^{b_2})\mu}{z_1(z_1-z_2)c_{10}^{a_2}c_{10}^{b_2}(\ln c_1^L-\ln c_1^R)}\\
&\quad+\frac{\mu}{2z_1(z_1-z_2)c_{10}^{b_2}}+\frac{(\beta_2-1)(\phi_0^{b_1}-\phi_0^{a_1})z_2\lambda}{(z_1-z_2)c_{10}^{b_2}}+\frac{(\beta_2-1)(\phi_0^{b_2}-\phi_0^{a_2})z_2\lambda\mu}{(z_1-z_2)c_{10}^{b_2}}
\end{aligned}
\tag{3.2}
$$

and

$$
\begin{aligned}
y_{11} &= \frac{[(\beta_1-1)c_1^L-\alpha_1 c_1^R](\phi_0^{a_1}-\phi_0^{b_1})}{z_1(z_2-z_1)c_{10}^{a_1}c_{10}^{b_1}(J_{10}+J_{20})}+\frac{(\beta_1-\alpha_1)c_1^L(\phi_0^{a_2}-\phi_0^{b_2})\mu}{z_1(z_2-z_1)c_{10}^{a_1}c_{10}^{b_1}(J_{10}+J_{20})}\\
&+\frac{(z_1J_{20}+z_2J_{10})(c_{10}^{a_1}-c_{10}^{b_1})}{z_1^2z_2(z_2-z_1)c_{10}^{a_1}c_{10}^{b_1}(J_{10}+J_{20})^2}+\frac{\phi_0^{a_1}-\phi_0^{b_1}+(\phi_0^{a_2}-\phi_0^{b_2})\mu}{z_1(z_2-z_1)(c_1^L-c_1^R)(J_{10}+J_{20})}\ln\frac{c_{10}^{b_1,m}}{c_{10}^{a_1,m}},\\
y_{21} &= \frac{[(\beta_2-1)c_1^L-\alpha_2 c_1^R](\phi_0^{a_2}-\phi_0^{b_2})\mu}{z_1(z_2-z_1)c_{10}^{a_2}c_{10}^{b_2}(J_{10}+J_{20})}+\frac{(\beta_2-\alpha_2)c_1^R(\phi_0^{a_1}-\phi_0^{b_1})}{z_1(z_2-z_1)c_{10}^{a_2}c_{10}^{b_2}(J_{10}+J_{20})}\\
&+\frac{(z_1J_{20}+z_2J_{10})(c_{10}^{a_2}-c_{10}^{b_2})\mu}{z_1^2z_2(z_2-z_1)c_{10}^{a_2}c_{10}^{b_2}(J_{10}+J_{20})^2}+\frac{\phi_0^{a_1}-\phi_0^{b_1}+(\phi_0^{a_2}-\phi_0^{b_2})\mu}{z_1(z_2-z_1)(c_1^L-c_1^R)(J_{10}+J_{20})}\ln\frac{c_{10}^{b_2,m}}{c_{10}^{a_2,m}},\\
J_{11} &= \frac{A_1[1+(1-B_1)z_2\lambda](1+z_1\lambda)}{(z_1-z_2)H(1)}+\frac{A_2[1+(1-B_2)z_2\lambda](1+z_1\lambda)\mu}{(z_1-z_2)H(1)},\\
J_{21} &= \frac{A_1[1+(1-B_1)z_1\lambda](1+z_2\lambda)}{(z_2-z_1)H(1)}+\frac{A_2[1+(1-B_2)z_1\lambda](1+z_2\lambda)\mu}{(z_2-z_1)H(1)},
\end{aligned}
\tag{3.3}
$$

where

$$
\begin{aligned}
\lambda &= \frac{\phi^L-\phi^R}{\ln c_1^L-\ln c_1^R}, A_1=\frac{(c_{10}^{b_1}-c_{10}^{a_1})(c_1^L-c_1^R)}{c_{10}^{a_1}c_{10}^{b_1}(\ln c_1^L-\ln c_1^R)},\\
B_1 &= \frac{\ln c_{10}^{b_1}-\ln c_{10}^{a_1}}{A_1}=\frac{c_{10}^{a_1}c_{10}^{b_1}(\ln c_1^L-\ln c_1^R)(\ln c_{10}^{b_1}-\ln c_{10}^{a_1})}{(c_{10}^{b_1}-c_{10}^{a_1})(c_1^L-c_1^R)},\\
A_2 &= \frac{(c_{10}^{b_2}-c_{10}^{a_2})(c_1^L-c_1^R)}{c_{10}^{a_2}c_{10}^{b_2}(\ln c_1^L-\ln c_1^R)},\\
B_2 &= \frac{\ln c_{10}^{b_2}-\ln c_{10}^{a_2}}{A_2}=\frac{c_{10}^{a_2}c_{10}^{b_2}(\ln c_1^L-\ln c_1^R)(\ln c_{10}^{b_2}-\ln c_{10}^{a_2})}{(c_{10}^{b_2}-c_{10}^{a_2})(c_1^L-c_1^R)}.
\end{aligned}
\tag{3.4}
$$

Proof. The proof is given in the appendix.

Remark 3.5. *It can be seen that as $Q_1 = 0$ or $Q_2 = 0$ in (1.8), the formulae for J_{11} and J_{21} in Proposition 3.4 are the same as those in [1].*

4. Effects of permanent charge and channel geometry

In this section, we study effects of permanent charges and channel geometry on individual flux and on $I - V$ relations under electroneutrality conditions:

$$
z_1L_1 = -z_2L_2 = L, \text{ and } z_1R_1 = -z_2R_2 = R. \tag{4.1}
$$

For small $|Q|$, the flux $\mathcal{J}_i$ of the ith ion species and the current $\mathcal{I}$ are

$$\mathcal{J}_i = D_i J_{i0} + D_i J_{i1} Q + O(Q^2),\ \mathcal{I} = \mathcal{I}_0 + \mathcal{I}_1 Q + O(Q^2), i = 1, 2, \tag{4.2}$$

where

$$\mathcal{I}_0 = z_1 D_1 J_{10} + z_2 D_2 J_{20} \text{ and } \mathcal{I}_1 = z_1 D_1 J_{11} + z_2 D_2 J_{21}. \tag{4.3}$$

The quantities J_{11} and J_{21} will be used to analyze the dominating effects of permanent charges and channel geometry on the ionic flow.

4.1. A comparison between zeroth-order and first-order in Q

For the ith ion species, $i = 1, 2$, denote the difference of its electrochemical potentials at the two boundaries by

$$\mu_i^\delta = \mu_i^\delta(V, L_i, R_i) = \mu_i(0) - \mu_i(1) = k_B T(z_i V + \ln L_i - \ln R_i). \tag{4.4}$$

Under the electroneutrality condition (4.1), from Corollary 3.3,

$$\begin{aligned} J_{10} &= \frac{L - R}{z_1 H(1)(\ln L - \ln R)} \frac{\mu_1^\delta}{k_B T} = \frac{L_1 - R_1}{H(1)(\ln L_1 - \ln R_1)} \frac{\mu_1^\delta}{k_B T}, \\ J_{20} &= \frac{R - L}{z_2 H(1)(\ln L - \ln R)} \frac{\mu_2^\delta}{k_B T} = \frac{L_2 - R_2}{H(1)(\ln L_2 - \ln R_2)} \frac{\mu_2^\delta}{k_B T}. \end{aligned} \tag{4.5}$$

Also, it follows from Proposition 3.4 that

$$\begin{aligned} J_{11} &= \Big(\frac{A_1[(1 - B_1) z_2 V + \ln L - \ln R]}{(z_1 - z_2) H(1)(\ln L - \ln R)^2} \\ &\quad + \frac{A_2[(1 - B_2) z_2 V + \ln L - \ln R]\mu}{(z_1 - z_2) H(1)(\ln L - \ln R)^2} \Big) \frac{\mu_1^\delta}{k_B T}, \\ J_{21} &= \Big(\frac{A_1[(1 - B_1) z_1 V + \ln L - \ln R]}{(z_2 - z_1) H(1)(\ln L - \ln R)^2} \\ &\quad + \frac{A_2[(1 - B_2) z_1 V + \ln L - \ln R]\mu}{(z_2 - z_1) H(1)(\ln L - \ln R)^2} \Big) \frac{\mu_2^\delta}{k_B T}, \end{aligned} \tag{4.6}$$

where $\alpha_1, \alpha_2, \beta_1, \beta_2$ are defined in (1.9), and A_1, A_2, B_1, B_2 defined in (3.4) become

$$
\begin{aligned}
A_1(L,R) &= -\frac{(\beta_1-\alpha_1)(L-R)^2}{[(1-\alpha_1)L+\alpha_1R][(1-\beta_1)L+\beta_1R](\ln L-\ln R)},\\
B_1(L,R) &= \frac{\ln[(1-\beta_1)L+\beta_1R]-\ln[(1-\alpha_1)L+\alpha_1R]}{A_1},\\
A_2(L,R) &= -\frac{(\beta_2-\alpha_2)(L-R)^2}{[(1-\alpha_2)L+\alpha_2R][(1-\beta_2)L+\beta_2R](\ln L-\ln R)},\\
B_2(L,R) &= \frac{\ln[(1-\beta_2)L+\beta_2R]-\ln[(1-\alpha_2)L+\alpha_2R]}{A_2}.
\end{aligned}
\tag{4.7}
$$

Lemma 4.1. *The quantities $A_1 = A_1(L,R), B_1 = B_1(L,R), A_2 = A_2(L,R), B_2 = B_2(L,R)$, and $\mu_i^\delta(V;L,R)$ scale invariantly in (L,R); that is, for any $s > 0$,*

$$
\begin{aligned}
&A_1(sL,sR) = A_1(L,R), B_1(sL,sR) = B_1(L,R), A_2(sL,sR) = A_2(L,R),\\
&B_2(sL,sR) = B_2(L,R) \text{ and } \mu_i^\delta(V;sL,sR) = \mu_i^\delta(V;L,R).
\end{aligned}
$$

Lemma 4.2. *The quantities $J_{i0}(V;L,R)$ and $\mathcal{I}_0(V;L,R)$ scale linearly in (L,R), and $J_{i1}(V;L,R)$ and $\mathcal{I}_1(V;L,R)$ scale invariantly in (L,R); that is, for any $s > 0$,*

$$
\begin{aligned}
&J_{i0}(V;sL,sR) = sJ_{i0}(V;L,R),\quad \mathcal{I}_0(V;sL,sR) = s\mathcal{I}_0(V;L,R),\\
&J_{i1}(V;sL,sR) = J_{i1}(V;L,R),\quad \mathcal{I}_1(V;sL,sR) = \mathcal{I}_1(V;L,R).
\end{aligned}
$$

For convenience, the following function is introduced in [1] and is useful below. For $t > 0$, Let

$$
\gamma(t) = \frac{t\ln t - t + 1}{(t-1)\ln t} \text{ for } t \neq 1 \text{ and } \gamma(1) = \frac{1}{2}. \tag{4.8}
$$

The following lemma was established in [1].

Lemma 4.3. *For $t > 0, 0 < \gamma(t) < 1, \gamma'(t) > 0, \lim\limits_{t\to 0}\gamma(t) = 0, \lim\limits_{t\to+\infty}\gamma(t) = 1$.*

4.2. Dependence of the signs of J_{11} and J_{21} on channel geometry

In this section, the signs of $J_{11}J_{10}$ and $J_{21}J_{20}$ will be determined by the channel geometry $(\alpha_1,\beta_1,\alpha_2,\beta_2)$ and the boundary condition (V,L,R).

Lemma 4.4. *Assume $z_1 > 0 > z_2$. Then, A_1, A_2, and $R - L$ have the same sign.*

Proof. This follows from the formulae for A_1 and A_2 in (4.7).

Due to the fact that $0 \le \alpha_i \le \beta_i \le 1$, and $i = 1, 2$, the following lemma was established in [1].

Lemma 4.5. *Let $t = \frac{L}{R}$, and let $\gamma(t)$ be as in (4.8). Then, $B_i > 0$ and $\lim_{t\to 1} B_i = 1$.*

For $t > 1$, the following hold:

(i) If $\alpha_i < \gamma(t)$, then there exists a unique $\beta_i^* \in (\alpha_i, 1)$ such that

$$1 - B_i < 0, \ for\, \beta_i \in (\alpha_i, \beta_i^*) \ and \ 1 - B_i > 0 \ for\, \beta_i \in (\beta_i^*, 1).$$

(ii) If $\alpha_i \ge \gamma(t)$, then $1 - B_i > 0$.

For $t < 1$, the following hold:

(iii) If $1 - \beta_i < \gamma(\frac{1}{t})$, then there exists a unique $\alpha_i^* \in (0, \beta_i)$ such that

$$1 - B_i < 0, \ for\, \alpha_i \in (\alpha_i^*, \beta_i) \ and \ 1 - B_i > 0 \ for\, \alpha_i \in (0, \alpha_i^*).$$

(iv) If $1 - \beta_i \ge \gamma(\frac{1}{t})$, then $1 - B_i > 0$.

From (1.9), it can be seen that $0 \le \alpha_1 \le \beta_1 \le \alpha_2 \le \beta_2 \le 1$; thus, the following result can be established.

Lemma 4.6. *Let $t = \frac{L}{R}$. Then, $B_1 - B_2 > 0$ for $t > 1$, and $B_1 - B_2 < 0$ for $t < 1$.*

Proof. We will justify that $B_1 - B_2 > 0$ for $t > 1$. The statement that $B_1 - B_2 < 0$ for $t < 1$ can be justified in a similar way. Let

$$\begin{aligned} g(\beta_2) = &\Big((1-\alpha_2)t + \alpha_2\Big)\Big((1-\beta_2)t + \beta_2\Big) \ln t \ln \frac{(1-\beta_2)t + \beta_2}{(1-\alpha_2)t + \alpha_2}(\beta_1 - \alpha_1) \\ &- \Big((1-\alpha_1)t + \alpha_1\Big)\Big((1-\beta_1)t + \beta_1\Big) \ln t \ln \frac{(1-\beta_1)t + \beta_1}{(1-\alpha_1)t + \alpha_1}(\beta_2 - \alpha_2). \end{aligned}$$

Then, we have

$$B_1 - B_2 = \frac{g(\beta_2)}{(\beta_2 - \alpha_2)(\beta_1 - \alpha_1)(t-1)^2}.$$

Obviously, $B_1 - B_2$ has the same sign as that of $g(\beta_2)$. Note that $\lim_{\beta_2 \to \alpha_2} g(\beta_2) = 0$. By calculation, one has

$$\begin{aligned} g'(\beta_2) = &\Big((1-\alpha_2)t + \alpha_2\Big)(1-t) \ln t \ln \frac{(1-\beta_2)t + \beta_2}{(1-\alpha_2)t + \alpha_2}(\beta_1 - \alpha_1) \\ &+ \Big((1-\alpha_2)t + \alpha_2\Big) \ln t \cdot (1-t)(\beta_1 - \alpha_1) \\ &- \Big((1-\alpha_1)t + \alpha_1\Big)\Big((1-\beta_1)t + \beta_1\Big) \ln t \ln \frac{(1-\beta_1)t + \beta_1}{(1-\alpha_1)t + \alpha_1}, \end{aligned}$$

$$g''(\beta_2) = \frac{(1-\alpha_2)t+\alpha_2}{(1-\beta_2)t+\beta_2}(1-t)^2 \ln t \cdot (\beta_1 - \alpha_1).$$

Therefore, for $t > 1$, the function $g(\beta_2)$ is concave upward. Let

$$\begin{aligned} f(\beta_1) = &\Big((1-\alpha_2)t+\alpha_2\Big)\ln t \cdot (1-t)(\beta_1-\alpha_1) \\ &- \Big((1-\alpha_1)t+\alpha_1\Big)\Big((1-\beta_1)t+\beta_1\Big)\ln t \ln \frac{(1-\beta_1)t+\beta_1}{(1-\alpha_1)t+\alpha_1}. \end{aligned}$$

Then $\lim\limits_{\beta_2\to\alpha_2} g'(\beta_2) = f(\beta_1)$.

Note that $\lim\limits_{\beta_1\to\alpha_1} f(\beta_1) = 0$. By calculation, one has

$$\begin{aligned} f'(\beta_1) &= (\alpha_2-\alpha_1)\ln t \cdot (1-t)^2 \\ &\quad - \Big((1-\alpha_1)t+\alpha_1\Big)(1-t)\ln t \ln \frac{(1-\beta_1)t+\beta_1}{(1-\alpha_1)t+\alpha_1}, \\ f''(\beta_1) &= -\frac{(1-\alpha_1)t+\alpha_1}{(1-\beta_1)t+\beta_1}(1-t)^2 \ln t. \end{aligned}$$

Therefore, for $t > 1$, the function $f(\beta_1)$ is concave downward. Additionally, it can be verified that

$$\lim_{\beta_1\to\alpha_2} f(\beta_1) > 0 \text{ and } \lim_{\beta_1\to\alpha_1} f'(\beta_1) = (\alpha_2-\alpha_1)\ln t \cdot (1-t)^2 > 0, \text{ for } t > 1.$$

It follows that $\lim\limits_{\beta_2\to\alpha_2} g'(\beta_2) = f(\beta_1) \geq 0$. Hence, we have $g(\beta_2) > 0$ for $t > 1$, that is, $B_1 - B_2 > 0$ for $t > 1$.

Theorem 4.7. *Assume $B_2 = 1$ and $B_1 = 1$, where B_1 and B_2 are in (4.7).*

For $t = \dfrac{L}{R} \neq 1$ and $\mu < -\dfrac{A_1}{A_2}$, then $J_{10}J_{11} > 0$ and $J_{20}J_{21} < 0$;

for $t = \dfrac{L}{R} \neq 1$ and $\mu > -\dfrac{A_1}{A_2}$, then $J_{10}J_{11} < 0$ and $J_{20}J_{21} > 0$.

Equivalently, for $t = \dfrac{L}{R} \neq 1$ and $\mu < -\dfrac{A_1}{A_2}$, a small positive Q strengthens $|J_1|$; for $t = \dfrac{L}{R} \neq 1$ and $\mu > -\dfrac{A_1}{A_2}$, a small positive Q reduces $|J_1|$; for $t = \dfrac{L}{R} \neq 1$ and $\mu > -\dfrac{A_1}{A_2}$, a small positive Q strengthens $|J_2|$; and for $t = \dfrac{L}{R} \neq 1$ and $\mu < -\dfrac{A_1}{A_2}$, a small positive Q reduces $|J_2|$.

Proof. As $B_1 = 1$ and $B_2 = 1$, (4.6) reduces to

$$\begin{aligned} J_{11} &= \frac{(A_1 + A_2\mu)(\ln L - \ln R)}{(z_1 - z_2)H(1)(\ln L - \ln R)^2} \frac{\mu_1^\delta}{k_B T}, \\ J_{21} &= \frac{(A_1 + A_2\mu)(\ln L - \ln R)}{(z_2 - z_1)H(1)(\ln L - \ln R)^2} \frac{\mu_2^\delta}{k_B T}. \end{aligned} \tag{4.9}$$

From (4.5), it follows that

$$\begin{aligned} J_{10}J_{11} &= \frac{(L - R)(A_1 + A_2\mu)(\mu_1^\delta)^2}{z_1(z_1 - z_2)[H(1)]^2(\ln L - \ln R)^2(k_B T)^2}, \\ J_{20}J_{21} &= \frac{(R - L)(A_1 + A_2\mu)(\mu_2^\delta)^2}{z_2(z_2 - z_1)[H(1)]^2(\ln L - \ln R)^2(k_B T)^2}. \end{aligned} \tag{4.10}$$

From (4.10), the result follows.

Theorem 4.8. *Assume $B_2 = 1$ and $B_1 \neq 1$, where B_2 and B_1 are in (4.7). Let V_q^1 and V_q^2 be as follows:*

$$\begin{aligned} V_q^1 &= V_q^1(L, R) = -\frac{(A_1 + A_2\mu)(\ln L - \ln R)}{z_2 A_1(1 - B_1)}, \\ V_q^2 &= V_q^2(L, R) = -\frac{(A_1 + A_2\mu)(\ln L - \ln R)}{z_1 A_1(1 - B_1)}. \end{aligned} \tag{4.11}$$

For $A_1(1 - B_1) > 0$ and $V < V_q^1$, then $J_{10}J_{11} > 0$;
for $A_1(1 - B_1) > 0$ and $V > V_q^1$, then $J_{10}J_{11} < 0$;
for $A_1(1 - B_1) < 0$ and $V < V_q^1$, then $J_{10}J_{11} < 0$;
for $A_1(1 - B_1) < 0$ and $V > V_q^1$, then $J_{10}J_{11} > 0$;
for $A_1(1 - B_1) > 0$ and $V < V_q^2$, then $J_{20}J_{21} > 0$;
for $A_1(1 - B_1) > 0$ and $V > V_q^2$, then $J_{20}J_{21} < 0$;
for $A_1(1 - B_1) < 0$ and $V < V_q^2$, then $J_{20}J_{21} < 0$;
for $A_1(1 - B_1) < 0$ and $V > V_q^2$, then $J_{20}J_{21} > 0$.

Equivalently, for $A_1(1 - B_1) > 0$ and $V < V_q^1$, or $A_1(1 - B_1) < 0$ and $V > V_q^1$, a small positive Q strengthens $|J_1|$; for $A_1(1 - B_1) > 0$ and $V > V_q^1$, or $A_1(1 - B_1) < 0$ and $V < V_q^1$, a small positive Q reduces $|J_1|$; for $A_1(1 - B_1) > 0$ and $V < V_q^2$, or $A_1(1 - B_1) < 0$ and $V > V_q^2$, a small positive Q strengthens $|J_2|$; and for $A_1(1 - B_1) > 0$ and $V > V_q^2$, or $A_1(1 - B_1) < 0$ and $V < V_q^2$, a small positive Q reduces $|J_2|$.

Proof. As $B_2 = 1$ and $B_1 \neq 1$, (4.6) reduces to

$$\begin{aligned} J_{11} &= \frac{A_1(1-B_1)z_2V + (A_1 + A_2\mu)(\ln L - \ln R)}{(z_1 - z_2)H(1)(\ln L - \ln R)^2} \frac{\mu_1^\delta}{k_B T}, \\ J_{21} &= \frac{A_1(1-B_1)z_1V + (A_1 + A_2\mu)(\ln L - \ln R)}{(z_2 - z_1)H(1)(\ln L - \ln R)^2} \frac{\mu_2^\delta}{k_B T}. \end{aligned} \tag{4.12}$$

From (4.5), it follows that

$$\begin{aligned} J_{10}J_{11} &= \frac{(L-R)[A_1(1-B_1)z_2V + (A_1 + A_2\mu)(\ln L - \ln R)](\mu_1^\delta)^2}{z_1(z_1 - z_2)[H(1)]^2(\ln L - \ln R)^3(k_B T)^2}, \\ J_{20}J_{21} &= \frac{(R-L)[A_1(1-B_1)z_1V + (A_1 + A_2\mu)(\ln L - \ln R)](\mu_2^\delta)^2}{z_2(z_2 - z_1)[H(1)]^2(\ln L - \ln R)^3(k_B T)^2}. \end{aligned} \tag{4.13}$$

From (4.13), the result follows.

Remark 4.9. *The signs of $A_1(1-B_1)$ can be determined by Lemmas 4.4 and 4.5.*

Lemma 4.10. *Assume $B_2 \neq 1$, where B_2 is in (4.7).*

For $1-B_2 > 0, t > 1, \mu < -\dfrac{A_1(1-B_1)}{A_2(1-B_2)}$, then $A_1(1-B_1) + A_2(1-B_2)\mu > 0$;

for $1-B_2 > 0, t > 1, \mu > -\dfrac{A_1(1-B_1)}{A_2(1-B_2)}$, then $A_1(1-B_1) + A_2(1-B_2)\mu < 0$;

for $1-B_2 > 0, t < 1, \mu > -\dfrac{A_1(1-B_1)}{A_2(1-B_2)}$, then $A_1(1-B_1) + A_2(1-B_2)\mu > 0$;

for $1-B_2 > 0, t < 1, \mu < -\dfrac{A_1(1-B_1)}{A_2(1-B_2)}$, then $A_1(1-B_1) + A_2(1-B_2)\mu < 0$;

for $1-B_2 < 0, t > 1, \mu > -\dfrac{A_1(1-B_1)}{A_2(1-B_2)}$, then $A_1(1-B_1) + A_2(1-B_2)\mu > 0$;

for $1-B_2 < 0, t > 1, \mu < -\dfrac{A_1(1-B_1)}{A_2(1-B_2)}$, then $A_1(1-B_1) + A_2(1-B_2)\mu < 0$;

for $1-B_2 < 0, t < 1, \mu < -\dfrac{A_1(1-B_1)}{A_2(1-B_2)}$, then $A_1(1-B_1) + A_2(1-B_2)\mu > 0$;

for $1-B_2 < 0, t < 1, \mu > -\dfrac{A_1(1-B_1)}{A_2(1-B_2)}$, then $A_1(1-B_1) + A_2(1-B_2)\mu < 0$.

Proof. For $1-B_2 > 0, t > 1$, it follows from Lemma 4.4 that $A_2 < 0$ and $A_2(1-B_2) < 0$. Therefore, as $\mu < -\dfrac{A_1(1-B_1)}{A_2(1-B_2)}$, then $A_1(1-B_1) + A_2(1-B_2)\mu > 0$. Other cases can be similarly verified.

Remark 4.11. *The signs of $1-B_2$ can be determined by Lemma 4.5.*

Theorem 4.12. *Assume $B_2 \neq 1$, where B_2 is in (4.7) and $A_1(1-B_1)+A_2(1-B_2)\mu \neq 0$. Let V_q^3 and V_q^4 be given by*

$$\begin{aligned} V_q^3 &= V_q^3(L,R) = -\frac{(A_1+A_2\mu)(\ln L-\ln R)}{z_2[A_1(1-B_1)+A_2(1-B_2)\mu]},\\ V_q^4 &= V_q^4(L,R) = -\frac{(A_1+A_2\mu)(\ln L-\ln R)}{z_1[A_1(1-B_1)+A_2(1-B_2)\mu]}. \end{aligned} \tag{4.14}$$

For $A_1(1-B_1)+A_2(1-B_2)\mu > 0$ and $V < V_q^3$, then $J_{10}J_{11} > 0$;
for $A_1(1-B_1)+A_2(1-B_2)\mu > 0$ and $V > V_q^3$, then $J_{10}J_{11} < 0$;
for $A_1(1-B_1)+A_2(1-B_2)\mu < 0$ and $V < V_q^3$, then $J_{10}J_{11} < 0$;
for $A_1(1-B_1)+A_2(1-B_2)\mu < 0$ and $V > V_q^3$, then $J_{10}J_{11} > 0$;
for $A_1(1-B_1)+A_2(1-B_2)\mu > 0$ and $V < V_q^4$, then $J_{20}J_{21} > 0$;
for $A_1(1-B_1)+A_2(1-B_2)\mu > 0$ and $V > V_q^4$, then $J_{20}J_{21} < 0$;
for $A_1(1-B_1)+A_2(1-B_2)\mu < 0$ and $V < V_q^4$, then $J_{20}J_{21} > 0$;
for $A_1(1-B_1)+A_2(1-B_2)\mu < 0$ and $V > V_q^4$, then $J_{20}J_{21} < 0$.

Equivalently, for $A_1(1-B_1)+A_2(1-B_2)\mu > 0$ and $V < V_q^3$, or $A_1(1-B_1)+A_2(1-B_2)\mu < 0$ and $V > V_q^3$, a small positive Q strengthens $|J_1|$; for $A_1(1-B_1)+A_2(1-B_2)\mu > 0$ and $V > V_q^3$, or $A_1(1-B_1)+A_2(1-B_2)\mu < 0$ and $V < V_q^3$, a small positive Q reduces $|J_1|$; for $A_1(1-B_1)+A_2(1-B_2)\mu > 0$ and $V < V_q^4$, or $A_1(1-B_1)+A_2(1-B_2)\mu < 0$ and $V < V_q^4$, a small positive Q strengthens $|J_2|$; and for $A_1(1-B_1)+A_2(1-B_2)\mu > 0$ and $V > V_q^4$, or $A_1(1-B_1)+A_2(1-B_2)\mu < 0$ and $V > V_q^4$, a small positive Q reduces $|J_2|$.

Proof. As $B_2 \neq 1$, based on (4.5) and (4.6), we have

$$J_{10}J_{11} = \frac{(L-R)(\mu_1^\delta)^2\Big([A_1(1-B_1)+A_2(1-B_2)\mu]z_2V+(A_1+A_2\mu)(\ln L-\ln R)\Big)}{z_1(z_1-z_2)[H(1)]^2(\ln L-\ln R)^3(k_BT)^2},$$

$$J_{20}J_{21} = \frac{(R-L)(\mu_2^\delta)^2\Big([A_1(1-B_1)+A_2(1-B_2)\mu]z_1V+(A_1+A_2\mu)(\ln L-\ln R)\Big)}{z_2(z_2-z_1)[H(1)]^2(\ln L-\ln R)^3(k_BT)^2}.$$

Therefore, the result follows.

Theorem 4.13. *Assume $B_2 \neq 1$, where B_2 is in (4.7) and $A_1(1-B_1)+A_2(1-B_2)\mu = 0$, that is, $\mu = -\dfrac{A_1(1-B_1)}{A_2(1-B_2)}$.*

For $t > 1$ and $1-B_2 > 0$, then $J_{10}J_{11} < 0$;
for $t > 1$ and $1-B_2 < 0$, then $J_{10}J_{11} > 0$;
for $t < 1$ and $1-B_2 > 0$, then $J_{10}J_{11} > 0$;
for $t < 1$ and $1-B_2 < 0$, then $J_{10}J_{11} < 0$;
for $t > 1$ and $1-B_2 > 0$, then $J_{20}J_{21} > 0$;

for $t > 1$ and $1 - B_2 < 0$, then $J_{20}J_{21} < 0$;

for $t < 1$ and $1 - B_2 > 0$, then $J_{20}J_{21} < 0$;

for $t < 1$ and $1 - B_2 < 0$, then $J_{20}J_{21} > 0$.

Equivalently, for $t > 1$ and $1 - B_2 < 0$, or $t < 1$ and $1 - B_2 > 0$, a small positive Q strengthens $|J_1|$; for $t > 1$ and $1 - B_2 > 0$, or $t < 1$ and $1 - B_2 < 0$, a small positive Q reduces $|J_1|$; for $t > 1$ and $1 - B_2 > 0$, or $t < 1$ and $1 - B_2 < 0$, a small positive Q strengthens $|J_2|$; and for $t > 1$ and $1 - B_2 < 0$, or $t < 1$ and $1 - B_2 > 0$, a small positive Q reduces $|J_2|$.

Proof. As $B_2 \neq 1$ and $\mu = -\dfrac{A_1(1 - B_1)}{A_2(1 - B_2)}$, (4.6) reduces to

$$\begin{aligned} J_{11} &= \frac{1}{(z_1 - z_2)H(1)(\ln L - \ln R)} \frac{\mu_1^\delta}{k_B T} \frac{A_1(B_1 - B_2)}{1 - B_2}, \\ J_{21} &= \frac{1}{(z_2 - z_1)H(1)(\ln L - \ln R)} \frac{\mu_2^\delta}{k_B T} \frac{A_1(B_1 - B_2)}{1 - B_2}. \end{aligned} \tag{4.15}$$

From (4.5), it follows that

$$\begin{aligned} J_{10}J_{11} &= \frac{(L - R)(\mu_1^\delta)^2}{z_1(z_1 - z_2)[H(1)]^2(\ln L - \ln R)^2(k_B T)^2} \frac{A_1(B_1 - B_2)}{1 - B_2}, \\ J_{20}J_{21} &= \frac{(R - L)(\mu_2^\delta)^2}{z_2(z_2 - z_1)[H(1)]^2(\ln L - \ln R)^2(k_B T)^2} \frac{A_1(B_1 - B_2)}{1 - B_2}. \end{aligned} \tag{4.16}$$

From (4.16) and Lemma 4.6, the result follows.

Remark 4.14. *Analytically, the effects of a small permanent charge Q on an individual flux are proved in Theorems 4.7, 4.8, 4.12, and 4.13, that is, a small positive Q can strengthens or reduce the individual flux $|J_1|$ or $|J_2|$.*

Proposition 4.15. *The potentials $V_q^1(L, R)$, $V_q^2(L, R)$, $V_q^3(L, R)$, and $V_q^4(L, R)$ scale invariantly in (L, R).*

Proof. It can be seen from Lemma 4.1 that A_1, A_2, B_1, and B_2 scale invariantly in (L, R). Then, based on the formulae for $V_q^1(L, R)$, $V_q^2(L, R)$ in (4.8) and $V_q^3(L, R)$, $V_q^4(L, R)$ in (4.14), Proposition 4.15 is proved.

4.3. Dependence of magnitudes of J_{11} and J_{21} on channel geometry

We now analyze how the magnitudes of J_{11} and J_{21} depend on the channel geometry $(\alpha_1, \beta_1, \alpha_2, \beta_2)$, and the boundary condition (V, L, R).

Recall that $(\alpha_1,\beta_1,\alpha_2,\beta_2)\in\Omega=\{0\le\alpha_1\le\beta_1\le\alpha_2\le\beta_2\le 1\}$, and

$$\begin{aligned} J_{11} &= \frac{p_1(\alpha_1,\beta_1,\alpha_2,\beta_2)}{(z_1-z_2)H(1)(\ln L-\ln R)^2}\cdot\frac{\mu_1^{\delta}(V;L,R)}{k_BT},\\ J_{21} &= \frac{p_2(\alpha_1,\beta_1,\alpha_2,\beta_2)}{(z_2-z_1)H(1)(\ln L-\ln R)^2}\cdot\frac{\mu_2^{\delta}(V;L,R)}{k_BT}, \end{aligned} \tag{4.17}$$

where

$$\begin{aligned} p_1(\alpha_1,\beta_1,\alpha_2,\beta_2) &= \frac{(\alpha_1-\beta_1)(L-R)^2(z_2V+\ln L-\ln R)}{[(1-\alpha_1)L+\alpha_1R][(1-\beta_1)L+\beta_1R](\ln L-\ln R)}\\ &\quad - z_2V\ln\frac{(1-\beta_1)L+\beta_1R}{(1-\alpha_1)L+\alpha_1R}\\ &\quad + \Big(\frac{(\alpha_2-\beta_2)(L-R)^2(z_2V+\ln L-\ln R)}{[(1-\alpha_2)L+\alpha_2R][(1-\beta_2)L+\beta_2R](\ln L-\ln R)}\\ &\quad - z_2V\ln\frac{(1-\beta_2)L+\beta_2R}{(1-\alpha_2)L+\alpha_2R}\Big)\mu,\\ p_2(\alpha_1,\beta_1,\alpha_2,\beta_2) &= \frac{(\alpha_1-\beta_1)(L-R)^2(z_1V+\ln L-\ln R)}{[(1-\alpha_1)L+\alpha_1R][(1-\beta_1)L+\beta_1R](\ln L-\ln R)}\\ &\quad - z_1V\ln\frac{(1-\beta_1)L+\beta_1R}{(1-\alpha_1)L+\alpha_1R}\\ &\quad + \Big(\frac{(\alpha_2-\beta_2)(L-R)^2(z_1V+\ln L-\ln R)}{[(1-\alpha_2)L+\alpha_2R][(1-\beta_2)L+\beta_2R](\ln L-\ln R)}\\ &\quad - z_1V\ln\frac{(1-\beta_2)L+\beta_2R}{(1-\alpha_2)L+\alpha_2R}\Big)\mu. \end{aligned} \tag{4.18}$$

Lemma 4.16. *Assume* $\gamma_1^*=\gamma(\frac{L}{R})-\frac{1}{z_2V}\in(0,1)$ *where* $\gamma(t)\in(0,1)$ *is defined in (4.8).*

(I1). For $0\le\mu\le 1$, $|p_1(\alpha_1,\beta_1,\alpha_2,\beta_2)|$ *attains its maximum at either* $(\gamma_1^*,1,1,1)$, *or* $(0,\gamma_1^*,\beta_2,\beta_2)$, *where* $\gamma_1^*\le\beta_2\le 1$.

(I2). For $\mu>1$, $|p_1(\alpha_1,\beta_1,\alpha_2,\beta_2)|$ *attains its maximum at either* $(0,0,0,\gamma_1^*)$, *or* $(\alpha_1,\alpha_1,\gamma_1^*,1)$, *where* $0\le\alpha_1\le\gamma_1^*$.

(I3). For $-1\le\mu<0$, $|p_1(\alpha_1,\beta_1,\alpha_2,\beta_2)|$ *attains its maximum at either* $(0,\gamma_1^*,\gamma_1^*,1)$, *or* $(\gamma_1^*,1,1,1)$.

(I4). For $\mu<-1$, $|p_1(\alpha_1,\beta_1,\alpha_2,\beta_2)|$ *attains its maximum at either* $(0,0,0,\gamma_1^*)$, *or* $(0,\gamma_1^*,\gamma_1^*,1)$. *Assume* $\gamma_1^*\notin(0,1)$.

(I5). For $|\mu|>1$, *then* $|p_1(\alpha_1,\beta_1,\alpha_2,\beta_2)|$ *attains its maximum at* $(0,0,0,1)$.

(I6). For $|\mu|\le 1$, *then* $|p_1(\alpha_1,\beta_1,\alpha_2,\beta_2)|$ *attains its maximum at* $(0,1,1,1)$.

Similarly, Assume $\gamma_2^* = \gamma(\frac{L}{R}) - \frac{1}{z_1 V} \in (0,1)$.

(II1). For $0 \le \mu \le 1$, $|p_2(\alpha_1,\beta_1,\alpha_2,\beta_2)|$ *attains its maximum at either* $(\gamma_2^*,1,1,1)$, *or* $(0,\gamma_2^*,\beta_2,\beta_2)$, *where* $\gamma_2^* \le \beta_2 \le 1$.

(II2). For $\mu > 1$, $|p_2(\alpha_1,\beta_1,\alpha_2,\beta_2)|$ *attains its maximum at either* $(0,0,0,\gamma_2^*)$, *or* $(\alpha_1,\alpha_1,\gamma_2^*,1)$, *where* $0 \le \alpha_1 \le \gamma_2^*$.

(II3). For $-1 \le \mu < 0$, $|p_2(\alpha_1,\beta_1,\alpha_2,\beta_2)|$ *attains its maximum at either* $(0,\gamma_2^*,\gamma_2^*,1)$, *or* $(\gamma_2^*,1,1,1)$.

(II4). For $\mu < -1$, $|p_2(\alpha_1,\beta_1,\alpha_2,\beta_2)|$ *attains its maximum at either* $(0,0,0,\gamma_2^*)$, *or* $(0,\gamma_2^*,\gamma_2^*,1)$. *Assume* $\gamma_2^* \notin (0,1)$.

(II5). For $|\mu| > 1$, $|p_2(\alpha_1,\beta_1,\alpha_2,\beta_2)|$ *attains its maximum at* $(0,0,0,1)$.

(II6). For $|\mu| \le 1$, $|p_2(\alpha_1,\beta_1,\alpha_2,\beta_2)|$ *attains its maximum at* $(0,1,1,1)$.

Proof. Note that

$$\begin{aligned}
\frac{\partial p_1(\alpha_1,\beta_1,\alpha_2,\beta_2)}{\partial \alpha_1} &= \frac{(L-R)^2(z_2V+\ln L-\ln R)}{[(1-\alpha_1)L+\alpha_1 R]^2(\ln L-\ln R)} \\
&\quad + z_2 V\frac{R-L}{(1-\alpha_1)L+\alpha_1 R}, \\
\frac{\partial p_1(\alpha_1,\beta_1,\alpha_2,\beta_2)}{\partial \beta_1} &= -\frac{(L-R)^2(z_2V+\ln L-\ln R)}{[(1-\beta_1)L+\beta_1 R]^2(\ln L-\ln R)} \\
&\quad - z_2 V\frac{R-L}{(1-\beta_1)L+\beta_1 R}, \\
\frac{\partial p_1(\alpha_1,\beta_1,\alpha_2,\beta_2)}{\partial \alpha_2} &= \Big(\frac{(L-R)^2(z_2V+\ln L-\ln R)}{[(1-\alpha_2)L+\alpha_2 R]^2(\ln L-\ln R)} \\
&\quad + z_2 V\frac{R-L}{(1-\alpha_2)L+\alpha_2 R}\Big)\mu, \\
\frac{\partial p_1(\alpha_1,\beta_1,\alpha_2,\beta_2)}{\partial \beta_2} &= -\Big(\frac{(L-R)^2(z_2V+\ln L-\ln R)}{[(1-\beta_2)L+\beta_2 R]^2(\ln L-\ln R)} \\
&\quad + z_2 V\frac{R-L}{(1-\beta_2)L+\beta_2 R}\Big)\mu.
\end{aligned} \tag{4.19}$$

Based on (4.19), it can be verified that any critical point of $p_1(\alpha_1,\beta_1,\alpha_2,\beta_2)$ satisfies the equality

$$\alpha_1 = \beta_1 = \alpha_2 = \beta_2.$$

Moreover, $p_1(\alpha_1,\beta_1,\alpha_2,\beta_2) = 0$ at any critical point $(\alpha_1,\beta_1,\alpha_2,\beta_2)$. Hence, the maximum of

$|p_1(\alpha_1,\beta_1,\alpha_2,\beta_2)|$ on Ω is attained on the boundary of Ω, which consists of the following five parts:

$$\begin{aligned}\{\alpha_1 = 0, 0 \le \beta_1 \le \alpha_2 \le \beta_2 \le 1\} &\cup \{\alpha_1 = \beta_1, 0 \le \alpha_1 \le \alpha_2 \le \beta_2 \le 1\}\\ &\cup \{\beta_1 = \alpha_2, 0 \le \alpha_1 \le \alpha_2 \le \beta_2 \le 1\}\\ &\cup \{\alpha_2 = \beta_2, 0 \le \alpha_1 \le \beta_1 \le \beta_2 \le 1\}\\ &\cup \{\beta_2 = 1, 0 \le \alpha_1 \le \beta_1 \le \alpha_2 \le 1\}.\end{aligned}$$

By analyzing the maximum of $|p_1(\alpha_1,\beta_1,\alpha_2,\beta_2)|$ on each part of the boundary of Ω, the result follows.

To illustrate some analytical results in Lemma 4.16, some numerical simulations on the maximum value of the function $|p_1(\alpha_1,\beta_1,\alpha_2,\beta_2)|$ are carried out in the following.

For $\mu = 0$, the function $|p_1(\alpha_1,\beta_1,\alpha_2,\beta_2)|$ in (4.18) reduces to a function in two variables α_1,β_1 of the following form:

$$\begin{aligned}p_1(\alpha_1,\beta_1,\alpha_2,\beta_2) = &\frac{(\alpha_1-\beta_1)(L-R)^2(z_2V+\ln L-\ln R)}{[(1-\alpha_1)L+\alpha_1R][(1-\beta_1)L+\beta_1R](\ln L-\ln R)}\\ &- z_2V\ln\frac{(1-\beta_1)L+\beta_1R}{(1-\alpha_1)L+\alpha_1R},\end{aligned} \tag{4.20}$$

where $0 \le \alpha_1 \le \beta_1 \le 1$, which is independent of α_2,β_2.

Actually, $\mu = 0$ corresponds to the case that the permanent charge $Q(x)$ takes the form of (1.5), that is, the permanent charge $Q(x)$ with one nonzero region, which has been analyzed in [1]. Moreover, it has been proved in [1] that

for $\gamma_1^* \in (0,1)$, $|p_1(\alpha_1,\beta_1,\alpha_2,\beta_2)|$ for $\mu = 0$ in (4.20) attains its maximum at either $(0,\gamma_1^*)$ or $(\gamma_1^*,1)$, and

for $\gamma_1^* \notin (0,1)$, $|p_1(\alpha_1,\beta_1,\alpha_2,\beta_2)|$ for $\mu = 0$ in (4.20) attains its maximum at $(0,1)$.

It can be seen that these results are consistent with those of $|p_1(\alpha_1,\beta_1,\alpha_2,\beta_2)|$ for $\mu = 0$ in (*I1*) and (*I6*), which are described in Lemma 4.16.

Because $|p_1(\alpha_1,\beta_1,\alpha_2,\beta_2)|$ for $\mu = 0$ in (4.20) is a function in two variables α_1,β_1, the graph of the function $|p_1(\alpha_1,\beta_1,\alpha_2,\beta_2)|$ for $\mu = 0$ in (4.20) can be visualized in three dimensional space. The graph of the function $|p_1(\alpha_1,\beta_1,\alpha_2,\beta_2)|$ for $\mu = 0$ in (4.20) is plotted in Figure 2, which supports these analytical results. Specifically, from Figure 2, it can be seen that

for $\gamma_1^* \in (0,1)$, $|p_1(\alpha_1,\beta_1,\alpha_2,\beta_2)|$ for $\mu = 0$ in (4.20) attains its maximum at either $(0,\gamma_1^*)$, and

for $\gamma_1^* \notin (0,1)$, $|p_1(\alpha_1,\beta_1,\alpha_2,\beta_2)|$ for $\mu = 0$ in (4.20) attains its maximum at $(0,1)$.

For $\mu \neq 0$, the domain of the function $|p_1(\alpha_1,\beta_1,\alpha_2,\beta_2)|$ in four variables, given in (4.18), is

$$\Omega = \{0 \le \alpha_1 \le \beta_1 \le \alpha_2 \le \beta_2 \le 1\}.$$

Therefore, to visualize the graph of the function $|p_1(\alpha_1,\beta_1,\alpha_2,\beta_2)|$ in (4.18) in three dimensional space, it is necessary to fix two variables, and α_2,β_2 are chosen to be fixed in our numerical simulations.

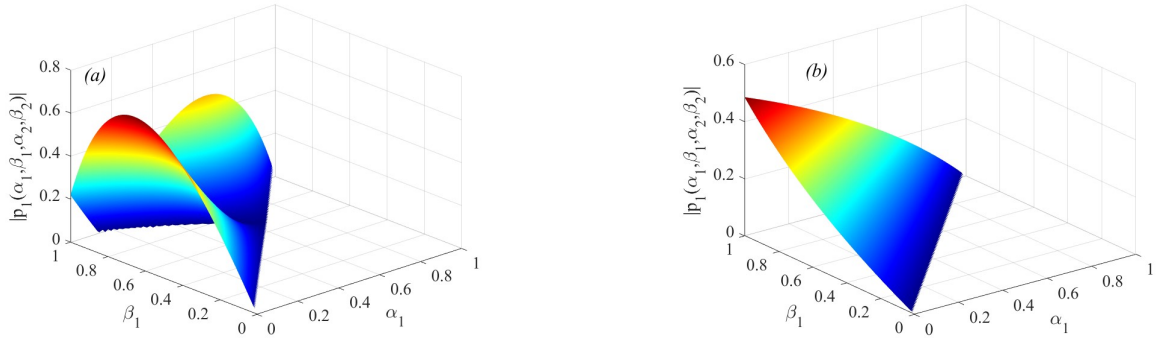

Figure 2. The parameters in image (a) are chosen as $L = 6, R = 3, z_2 = -1, V = 10$, and $\gamma_1^* = 0.6573 \in (0,1)$.The parameters in image (b) are chosen as $L = 6, R = 3, z_2 = -1, V = 0.5$, and $\gamma_1^* = 2.5573 \notin (0,1)$.

Fixing $\alpha_2 = \beta_2$, it can be seen that $|p_1(\alpha_1,\beta_1,\alpha_2,\beta_2)|$ in (4.18) also reduces to a function in two variables α_1,β_1 in (4.20), which is independent of μ. Therefore, the graph of the function $|p_1(\alpha_1,\beta_1,\alpha_2,\beta_2)|$ in (4.18) is the same as that in Figure 2, which is consistent with the analytical results in $(I1)$, $(I3)$, and $(I6)$, described in Lemma 4.16.

Fix $\alpha_2 < \beta_2$, and to demonstrate the influence of the parameter μ on the graph of the function $|p_1(\alpha_1,\beta_1,\alpha_2,\beta_2)|$ in (4.18), other parameters $L, R, z_2, V, \alpha_2, \beta_2$ are chosen to remain unchanged.

Fixing $L = 6, R = 3, z_2 = -1$, and $V = 10$, it follows that $\gamma_1^* = \gamma(\frac{L}{R}) - \frac{1}{z_2 V} = 0.6573 \in (0,1)$ by calculation, where $\gamma(t)$ is defined in (4.8). Also, fixing $\alpha_2 = \gamma_1^* = 0.6573, \beta_2 = 1$, the function $|p_1(\alpha_1,\beta_1,\alpha_2,\beta_2)|$ in (4.18) is plotted in Figure 3 by taking $\mu = 0.5, \mu = 2, \mu = -0.5$, and $\mu = -2$.

Image (b) for $\mu = 2$ in Figure 3 indicates $|p_1(\alpha_1,\beta_1,\alpha_2,\beta_2)|$ attains its maximum at $(\alpha_1,\alpha_1,\gamma_1^*,1)$, where $0 \le \alpha_1 \le \gamma_1^*$, which is consistent with the analytical results in $(I2)$ described in Lemma 4.16.

Images (c) and (d) for $\mu = -0.5$ and $\mu = -2$ in Figure 3 indicate that $|p_1(\alpha_1,\beta_1,\alpha_2,\beta_2)|$ attains its maximum at $(0,\gamma_1^*,\gamma_1^*,1)$, which is consistent with the analytical results in $(I3)$ and $(I4)$ described in Lemma 4.16. There is one difference between images (c) and (d) in Figure 3: The maximum value of $|p_1(\alpha_1,\beta_1,\alpha_2,\beta_2)|$ in image (c) is less than 1, but the maximum value of $|p_1(\alpha_1,\beta_1,\alpha_2,\beta_2)|$ in image (d) is greater than 1.6.

Moreover, it can be seen that images (a)–(d) in Figure 3 indicate that as the parameter μ changes, the maximum value of $|p_1(\alpha_1,\beta_1,\alpha_2,\beta_2)|$ changes accordingly.

To visualize the influence of the parameters α_2 and β_2 on the graph of the function $|p_1(\alpha_1,\beta_1,\alpha_2,\beta_2)|$ in (4.18), other parameters, L, R, z_2, V and μ, are chosen to be the same as those of Figure 3. Then. the graph of the function $|p_1(\alpha_1,\beta_1,\alpha_2,\beta_2)|$ in (4.18) is plotted in Figure 4 by fixing $\alpha_2 = 0.8$ and $\beta_2 = 0.9$. Also, the parameters α_2 and β_2 can be fixed to obtain other values belonging to the interval $[0,1]$.

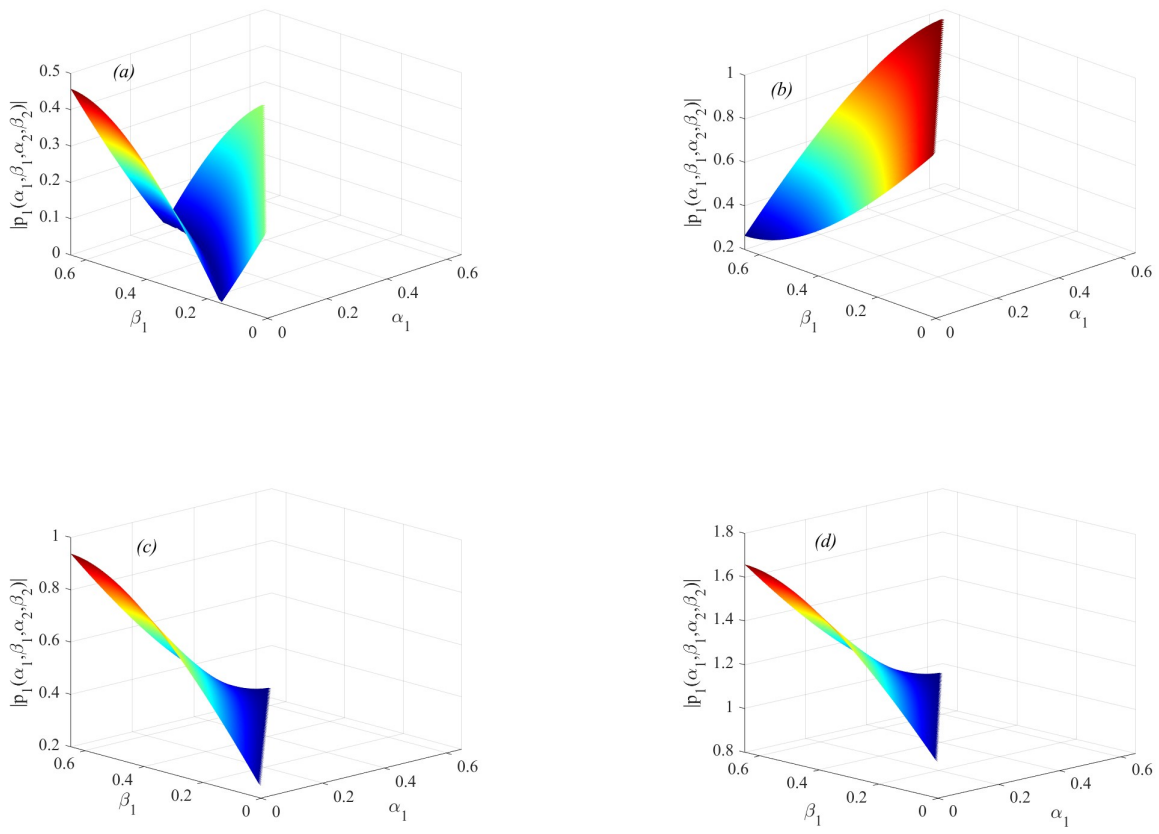

Figure 3. The parameters are chosen as $L = 6, R = 3, z_2 = -1, V = 10, \gamma_1^* = 0.6573, \alpha_2 = 0.6573$, and $\beta_2 = 1$. Images $(a), (b), (c), (d)$ correspond to $\mu = 0.5, \mu = 2, \mu = -0.5$, and $\mu = -2$, respectively.

Based on Lemma 4.16, the following results can be obtained.

Proposition 4.17. *The maximum of $|J_{11}|$ occurs in the same way as that of $|p_1(\alpha_1,\beta_1,\alpha_2,\beta_2)|$, and the maximum of $|J_{21}|$ occurs in the same way as that of $|p_2(\alpha_1,\beta_1,\alpha_2,\beta_2)|$.*

Proof. From the expressions for J_{11} and J_{21} in (4.17), it can be seen that choosing $\alpha_1, \beta_1, \alpha_2$, and β_2 as four independent variables and fixing other parameters, the conditions for the maximum of $|J_{11}|$ and $|J_{21}|$ are the same as those for the maximum of $|p_1(\alpha_1,\beta_1,\alpha_2,\beta_2)|$ and $|p_2(\alpha_1,\beta_1,\alpha_2,\beta_2)|$ in (4.18). Therefore, Proposition 4.17 is proved.

Remark 4.18. *As explained in [1], various conditions for the maximum of $|J_{i1}|$ are related to the structures of the ion channels.*

For example, in order to make $(\alpha_1,\beta_1,\alpha_2,\beta_2) \approx (0,0,0,1)$, $h(x)$ can take the following form: Namely, $b_2 - a_2 \ll 1$, and $h(x)$ for $x \in (a_2, b_2)$ is much smaller than $h(x)$ for $x \notin [a_2, b_2]$.

For another example, in order to make $(\alpha_1, \beta_1, \alpha_2, \beta_2) \approx (0, 1, 1, 1)$, $h(x)$ *can take the follwoing form: Namely,* $b_1 - a_1 \ll 1$, *and* $h(x)$ *for* $x \in (a_1, b_1)$ *is much smaller than* $h(x)$ *for* $x \notin [a_1, b_1]$.

These two cases both imply that the ion channels have a short and narrow cross-section. Similar explanations work for other conditions.

Remark 4.19. *The ratio* $\mu = \dfrac{Q_2}{Q_1}$ *is also a key parameter to determine the conditions for the maximum of* $|J_{i1}|$. *Moreover, when the parameter* μ *changes, the maximum point of* $|J_{i1}|$ *changes accordingly; therefore, the ratio* μ *can change the position of a short and narrow cross-section in ion channels.*

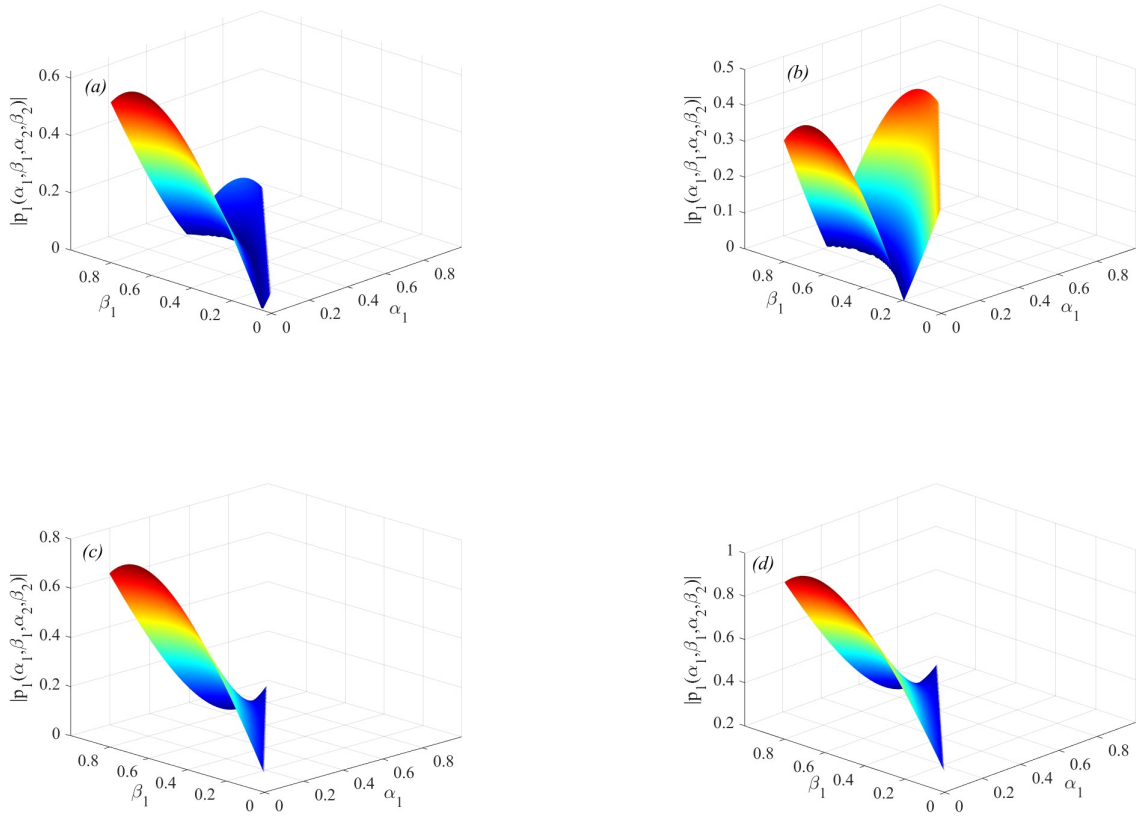

Figure 4. The parameters are chosen as $L = 6, R = 3, z_2 = -1, V = 10, \alpha_2 = 0.8$ and $\beta_2 = 0.9$. Images (a), (b), (c), and (d) correspond to $\mu = 0.5, \mu = 2, \mu = -0.5$, and $\mu = -2$, respectively.

4.4. Permanent charge effects on I-V relation

In this section, it is assumed that $A_i \neq 0$, and $i = 1, 2$.

It follows from (4.5) and (4.6) that

$$\mathcal{I}_0 = \frac{L-R}{H(1)(\ln L - \ln R)}\Big(D_1\frac{\mu_1^\delta}{k_BT} - D_2\frac{\mu_2^\delta}{k_BT}\Big),\ \mathcal{I}_1 = \frac{P(V;L,R)}{(z_1-z_2)H(1)}, \tag{4.21}$$

where $\lambda = \dfrac{V}{\ln L - \ln R}$ and

$$\begin{aligned} P = P(V;L,R) &= z_1z_2(z_1D_1 - z_2D_2)[A_1(1-B_1) + A_2(1-B_2)\mu]\lambda^2 \\ &+ \Big[z_1z_2(D_1-D_2)[A_1(1-B_1) + A_2(1-B_2)\mu] \\ &+ (z_1^2D_1 - z_2^2D_2)(A_1 + A_2\mu)\Big]\lambda + (z_1D_1 - z_2D_2)(A_1 + A_2\mu). \end{aligned} \tag{4.22}$$

Theorem 4.20. *For $Q = 0$, the zeroth order in ε approximation of the reversal potential V_{rev} is defined by*

$$V_{rev} = V_{rev}(L,R) = -\frac{D_1 - D_2}{z_1D_1 - z_2D_2}(\ln L - \ln R). \tag{4.23}$$

Hence, $\mathcal{I}_0 > 0$ if $V > V_{rev}$ and $\mathcal{I}_0 < 0$ if $V < V_{rev}$.

Proof. From the expressions for $\mathcal{I}_0$ in (4.21), it follows that

$$\mathcal{I}_0 = \frac{L-R}{H(1)(\ln L - \ln R)}\Big((z_1D_1 - z_2D_2)V + (D_1-D_2)(\ln L - \ln R)\Big). \tag{4.24}$$

Because $z_1D_1 - z_2D_2 > 0$, Theorem 4.20 is proved.

We now examine the sign of $\mathcal{I}_1$ to determine the leading effects of the permanent charge on the current.

Note that if $A_1(1-B_1) + A_2(1-B_2)\mu = 0$, then

$$\begin{aligned} \mathcal{I}_1 = \frac{1}{(z_1-z_2)H(1)(\ln L - \ln R)}\Big[&(z_1^2D_1 - z_2^2D_2)(A_1 + A_2\mu)V \\ &+ (z_1D_1 - z_2D_2)(A_1 + A_2\mu)(\ln L - \ln R)\Big]. \end{aligned} \tag{4.25}$$

Also, the assumption $A_1(1-B_1) + A_2(1-B_2)\mu = 0$ means (I): $B_2 = 1$ and $B_1 = 1$, or (II): $B_2 \neq 1$ and

$\mu = -\dfrac{A_1(1-B_1)}{A_2(1-B_2)}$.

For $z_1^2 D_1 - z_2^2 D_2 \neq 0$, let

$$V^0 = V^0(L,R) = -\frac{(z_1 D_1 - z_2 D_2)(\ln L - \ln R)}{z_1^2 D_1 - z_2^2 D_2}.$$

Lemma 4.21. *The signs of $A_1 + A_2\mu$ are collected in the following Table 2.*

Table 2. Signs of $A_1 + A_2\mu$.

Column 1	Column 2
If $t = \dfrac{L}{R} > 1, \mu < -\dfrac{A_1}{A_2}$, then $A_1 + A_2\mu > 0$	If $t = \dfrac{L}{R} < 1, \mu > -\dfrac{A_1}{A_2}$, then $A_1 + A_2\mu > 0$
If $t = \dfrac{L}{R} > 1, \mu > -\dfrac{A_1}{A_2}$, then $A_1 + A_2\mu < 0$	If $t = \dfrac{L}{R} < 1, \mu < -\dfrac{A_1}{A_2}$, then $A_1 + A_2\mu < 0$

Proof. If $t = \dfrac{L}{R} > 1$, it follows from Lemma 4.4 that $A_2 < 0$. Therefore, as $\mu > -\dfrac{A_1}{A_2}$, $A_1 + A_2\mu > 0$. Other cases can be similarly verified.

Theorem 4.22. *Assume $B_2 = 1$ and $B_1 = 1$.*

If $z_1^2 D_1 - z_2^2 D_2 = 0$, then $\mathcal{I}_1 > 0$ for $A_1 + A_2\mu > 0$ and $\mathcal{I}_1 < 0$ for $A_1 + A_2\mu < 0$.

If $\dfrac{(z_1^2 D_1 - z_2^2 D_2)(A_1 + A_2\mu)}{\ln L - \ln R} > 0$, then $\mathcal{I}_1 > 0$ for $V > V^0$ and $\mathcal{I}_1 < 0$ for $V < V^0$.

If $\dfrac{(z_1^2 D_1 - z_2^2 D_2)(A_1 + A_2\mu)}{\ln L - \ln R} < 0$, then $\mathcal{I}_1 > 0$ for $V < V^0$ and $\mathcal{I}_1 < 0$ for $V > V^0$.

Proof. Assume $B_2 = 1$ and $B_1 = 1$, then $A_1(1-B_1) + A_2(1-B_2)\mu = 0$, and the formula for $\mathcal{I}_1$ is given by (4.25). Based on the formula for $\mathcal{I}_1$ in (4.25), the statement of Theorem 4.22 can be verified.

Lemma 4.23. *Assume $B_2 \neq 1$ and $\mu = -\dfrac{A_1(1-B_1)}{A_2(1-B_2)}$.*

If $t = \dfrac{L}{R} \neq 1$ and $1 - B_2 > 0$, then $A_1 + A_2\mu < 0$.

If $t = \dfrac{L}{R} \neq 1$ and $1 - B_2 < 0$, then $A_1 + A_2\mu > 0$.

Proof. As $B_2 \neq 1$ and $\mu = -\dfrac{A_1(1-B_1)}{A_2(1-B_2)}$, then, one has

$$A_1 + A_2\mu = \frac{A_1(B_1 - B_2)}{1 - B_2}. \tag{4.26}$$

Based on (4.26) and Lemma 4.6, the result follows.

Theorem 4.24. *Assume* $B_2 \neq 1$ *and* $\mu = -\dfrac{A_1(1-B_1)}{A_2(1-B_2)}$.

If $z_1^2 D_1 - z_2^2 D_2 = 0$, *then* $\mathcal{I}_1 > 0$ *for* $A_1 + A_2\mu > 0$ *and* $\mathcal{I}_1 < 0$ *for* $A_1 + A_2\mu < 0$.

If $\dfrac{(z_1^2 D_1 - z_2^2 D_2)(A_1 + A_2\mu)}{\ln L - \ln R} > 0$, *then* $\mathcal{I}_1 > 0$ *for* $V > V^0$ *and* $\mathcal{I}_1 < 0$ *for* $V < V^0$.

If $\dfrac{(z_1^2 D_1 - z_2^2 D_2)(A_1 + A_2\mu)}{\ln L - \ln R} < 0$, *then* $\mathcal{I}_1 > 0$ *for* $V < V^0$ *and* $\mathcal{I}_1 < 0$ *for* $V > V^0$.

Proof. Assume $B_2 \neq 1$ and $\mu = -\dfrac{A_1(1-B_1)}{A_2(1-B_2)}$, then $A_1(1-B_1) + A_2(1-B_2)\mu = 0$, and the formula for $\mathcal{I}_1$ is given by (4.25). Based on the formula for $\mathcal{I}_1$ in (4.25), the statement of Theorem 4.22 can be verified.

Based on (4.22), if $A_1(1-B_1) + A_2(1-B_2)\mu \neq 0$, then $P = 0$ is a quadratic equation in λ whose discriminant is

$$\begin{aligned} \Delta = {} & z_1^2 z_2^2 (D_1 - D_2)^2 [A_1(1 - B_1 - r_-) \\ & + A_2(1 - B_2 - r_-)\mu][A_1(1 - B_1 - r_+) + A_2(1 - B_2 - r_+)\mu], \end{aligned} \tag{4.27}$$

where $r_- < r_+ \leq 0$ is given by

$$r_- = \frac{(z_1\sqrt{D_1} - z_2\sqrt{D_2})^2}{z_1 z_2(\sqrt{D_1} - \sqrt{D_2})^2} \text{ and } r_+ = \frac{(z_1\sqrt{D_1} + z_2\sqrt{D_2})^2}{z_1 z_2(\sqrt{D_1} + \sqrt{D_2})^2}. \tag{4.28}$$

Note that, if $D_1 = D_2$, then

$$r_- = -\infty \text{ and } r_+ = \frac{(z_1 + z_2)^2}{4 z_1 z_2}.$$

For convenience, let

$$\mu_1 = -\frac{A_1(1 - B_1 - r_-)}{A_2(1 - B_2 - r_-)}, \quad \mu_2 = -\frac{A_1(1 - B_1 - r_+)}{A_2(1 - B_2 - r_+)} \text{ and } \mu_3 = -\frac{A_1(1 - B_1)}{A_2(1 - B_2)}. \tag{4.29}$$

Note that if $r_+ = 0$, then $\mu_2 = \mu_3$.

Lemma 4.25. *Assume* $1 - B_2 = 0$.

If $t = \dfrac{L}{R} > 1$, *then* $A_1(1 - B_1) + A_2(1 - B_2)\mu > 0$ *for* $1 - B_1 < 0$ *and* $A_1(1 - B_1) + A_2(1 - B_2)\mu < 0$ *for* $1 - B_1 > 0$.

If $t = \dfrac{L}{R} < 1$, *then* $A_1(1 - B_1) + A_2(1 - B_2)\mu > 0$ *for* $1 - B_1 > 0$ *and* $A_1(1 - B_1) + A_2(1 - B_2)\mu < 0$ *for* $1 - B_1 < 0$.

Proof. If $t = \dfrac{L}{R} > 1$, it follows from Lemma 4.4 that $A_1 < 0$. Additionally, assume $1 - B_2 = 0$. Then $A_1(1-B_1)+A_2(1-B_2)\mu = A_1(1-B_1) > 0$ for $1 - B_1 < 0$, and $A_1(1-B_1)+A_2(1-B_2)\mu = A_1(1-B_1) < 0$ for $1 - B_1 > 0$. The other case can be verified similarly.

Remark 4.26. *As* $1 - B_2 \neq 0$, *the sign of* $A_1(1 - B_1) + A_2(1 - B_2)\mu$ *is determined by Lemma 4.10.*

Lemma 4.27. *(i) Assume* $r_- < 1 - B_2 < r_+$.

Then, $\mu_2 < \mu_3 < \mu_1$ *for* $t = \dfrac{L}{R} > 1$, *and* $\mu_1 < \mu_3 < \mu_2$ *for* $t = \dfrac{L}{R} < 1$.

(ii) Assume $1 - B_2 < r_-$.

Then, $\mu_1 < \mu_2 < \mu_3$ *for* $t = \dfrac{L}{R} > 1$, *and* $\mu_3 < \mu_2 < \mu_1$ *for* $t = \dfrac{L}{R} < 1$.

(iii) Assume $r_+ < 1 - B_2 < 0$.

Then, $\mu_3 < \mu_1 < \mu_2$ *for* $t = \dfrac{L}{R} > 1$, *and* $\mu_2 < \mu_1 < \mu_3$ *for* $t = \dfrac{L}{R} < 1$.

(iv) Assume $1 - B_2 > 0$.

Then, $\mu_1 < \mu_2 < \mu_3$ *for* $t = \dfrac{L}{R} > 1$, *and* $\mu_3 < \mu_2 < \mu_1$ *for* $t = \dfrac{L}{R} < 1$.

Proof. Note that

$$\begin{aligned}
\mu_1 - \mu_2 &= \frac{A_1(r_+ - r_-)(B_2 - B_1)}{A_2(1 - B_2 - r_+)(1 - B_2 - r_-)}, \\
\mu_3 - \mu_1 &= \frac{A_1 \cdot r_-(B_2 - B_1)}{A_2(1 - B_2 - r_-)(1 - B_2)}, \\
\mu_3 - \mu_2 &= \frac{A_1 \cdot r_+(B_2 - B_1)}{A_2(1 - B_2 - r_+)(1 - B_2)}.
\end{aligned} \tag{4.30}$$

Based on (4.30) and Lemma 4.6, the result follows.

Lemma 4.28. *Assume* $r_- < 1 - B_2 < r_+$.

If $t = \dfrac{L}{R} > 1$, *then* $\Delta > 0$ *for* $\mu_2 < \mu < \mu_1$, $\Delta < 0$ *for* $\mu > \mu_1$ *or* $\mu < \mu_2$, *and* $\Delta = 0$ *for* $\mu = \mu_1$ *or* $\mu = \mu_2$.

If $t = \dfrac{L}{R} < 1$, *then* $\Delta > 0$ *for* $\mu_1 < \mu < \mu_2$, $\Delta < 0$ *for* $\mu > \mu_2$ *or* $\mu < \mu_1$, *and* $\Delta = 0$ *for* $\mu = \mu_1$ *or* $\mu = \mu_2$.

Proof. Assume $r_- < 1 - B_2 < r_+$, then $1 - B_2 - r_- > 0$ and $1 - B_2 - r_+ < 0$.

If $t = \dfrac{L}{R} > 1$, it follows from Lemma 4.4 that $A_2 < 0$. Therefore, $A_2(1 - B_2 - r_-) < 0$ and $A_2(1 - B_2 - r_+) > 0$.

For $\mu_2 < \mu < \mu_1$, it follows from (4.29) that $-\dfrac{A_1(1 - B_1 - r_+)}{A_2(1 - B_2 - r_+)} < \mu < -\dfrac{A_1(1 - B_1 - r_-)}{A_2(1 - B_2 - r_-)}$. Therefore, $A_1(1 - B_1 - r_-) + A_2(1 - B_2 - r_-)\mu > 0$, and $A_1(1 - B_1 - r_+) + A_2(1 - B_2 - r_+)\mu > 0$. Based on the expression for Δ in (4.27), it can be seen that $\Delta > 0$.

Other cases can be verified similarly.

Lemma 4.29. *Assume* $1 - B_2 \notin [r_-, r_+]$.

If $t = \dfrac{L}{R} > 1$, *then* $\Delta < 0$ *for* $\mu_1 < \mu < \mu_2$, $\Delta > 0$ *for* $\mu > \mu_2$ *or* $\mu < \mu_1$, *and* $\Delta = 0$ *for* $\mu = \mu_1$ *or* $\mu = \mu_2$.

If $t = \dfrac{L}{R} < 1$, *then* $\Delta < 0$ *for* $\mu_2 < \mu < \mu_1$, $\Delta > 0$ *for* $\mu > \mu_1$ *or* $\mu < \mu_2$, *and* $\Delta = 0$ *for* $\mu = \mu_1$ *or* $\mu = \mu_2$.

Proof. The proof of Lemma 4.29 is similar to that of Lemma 4.28.

Lemma 4.30. *Assume* $1 - B_2 = r_-$.

If $t = \dfrac{L}{R} > 1$, *then* $\Delta < 0$ *for* $\mu < \mu_2$, $\Delta > 0$ *for* $\mu > \mu_2$, *and* $\Delta = 0$ *for* $\mu = \mu_2$.

If $t = \dfrac{L}{R} < 1$, *then* $\Delta < 0$ *for* $\mu > \mu_2$, $\Delta > 0$ *for* $\mu < \mu_2$, *and* $\Delta = 0$ *for* $\mu = \mu_2$.

Proof. Assume $1 - B_2 = r_-$, then $1 - B_2 - r_- = 0$. From (4.28), it can be seen that $r_- < r_+$. Therefore, $1 - B_2 - r_+ < 0$.

If $t = \dfrac{L}{R} > 1$, it follows from Lemma 4.4 that $A_1 < 0$ and $A_2 < 0$. Therefore, $A_2(1 - B_2 - r_+) > 0$.

If $t = \dfrac{L}{R} > 1$, it follows from Lemma 4.6 that $-B_1 < -B_2$. Therefore, $1 - B_1 - r_- < 0$.

For $\mu < \mu_2$, it follows from (4.29) that $\mu < -\dfrac{A_1(1 - B_1 - r_+)}{A_2(1 - B_2 - r_+)}$. Therefore, $A_1(1 - B_1 - r_+) + A_2(1 - B_2 - r_+)\mu < 0$. Based on the expression for Δ in (4.27), it can be seen that $\Delta < 0$.

Other cases can be verified similarly.

Lemma 4.31. *Assume* $1 - B_2 = r_+$.

If $t = \dfrac{L}{R} > 1$, *then* $\Delta < 0$ *for* $\mu > \mu_1$, $\Delta > 0$ *for* $\mu < \mu_1$, *and* $\Delta = 0$ *for* $\mu = \mu_1$.

If $t = \dfrac{L}{R} < 1$, *then* $\Delta < 0$ *for* $\mu < \mu_1$, $\Delta > 0$ *for* $\mu > \mu_1$, *and* $\Delta = 0$ *for* $\mu = \mu_1$.

Proof. The proof of Lemma 4.31 is similar to that of Lemma 4.30.

Remark 4.32. *In Lemmas 4.28–4.31, conditions in terms of* $1 - B_2$ *can be made in terms of* α_2, β_2, L *and* R *by using Lemma 4.5.*

Theorem 4.33. *For the sign of* $\mathcal{I}_1$ *in (4.21), one has the following results:*

(i) If $\Delta < 0$*, then* $\mathcal{I}_1 < 0$ *for* $A_1(1-B_1)+A_2(1-B_2)\mu > 0$ *and* $\mathcal{I}_1 > 0$ *for* $A_1(1-B_1)+A_2(1-B_2)\mu < 0$.

(ii) If $\Delta = 0$*, then there exists one potential* $V_q^0 = V_q^0(L,R)$ *such that*

(ii1) if $V = V_q^0$*, then* $\mathcal{I}_1 = 0$*;*

(ii2) if $V \neq V_q^0$*, then* $\mathcal{I}_1 < 0$ *for* $A_1(1-B_1)+A_2(1-B_2)\mu > 0$ *and* $\mathcal{I}_1 > 0$ *for* $A_1(1-B_1)+A_2(1-B_2)\mu < 0$.

(iii) If $\Delta > 0$*, then there exist two potentials* $V_q^{\pm} = V_q^{\pm}(L,R)$ *such that*

(iii1) if $V = V_q^{\pm}$*, then* $\mathcal{I}_1 = 0$*;*

(iii2) if $V \in (V_q^-, V_q^+)$*, then* $\mathcal{I}_1 > 0$ *for* $A_1(1-B_1) + A_2(1-B_2)\mu > 0$ *and* $\mathcal{I}_1 < 0$ *for* $A_1(1-B_1) + A_2(1-B_2)\mu < 0$*;*

(iii3) if $V \notin [V_q^-, V_q^+]$*, then* $\mathcal{I}_1 < 0$ *for* $A_1(1-B_1) + A_2(1-B_2)\mu > 0$ *and* $\mathcal{I}_1 > 0$ *for* $A_1(1-B_1) + A_2(1-B_2)\mu < 0$.

Proof. From (4.21) and (4.22), it can be seen that $\mathcal{I}_1$ is a quadratic equation in V by fixing other parameters, and its discriminant Δ is given by (4.27). Therefore, based on (4.21) and (4.22), if $\Delta < 0$, then $\mathcal{I}_1 < 0$ for $A_1(1-B_1) + A_2(1-B_2)\mu > 0$ and an arbitrary V; if $\Delta < 0$, then $\mathcal{I}_1 > 0$ for $A_1(1-B_1) + A_2(1-B_2)\mu < 0$ and an arbitrary V.

Other cases can be verified similarly.

Remark 4.34. *The sign of* $A_1(1-B_1) + A_2(1-B_2)\mu$ *in Theorem 4.33 is determined by Lemmas 4.10 and 4.25. The sign of* Δ *in Theorem 4.33 is determined by Lemmas 4.28–4.31.*

Remark 4.35. *In summary, the effects of a small permanent charge on the I-V relation are analytically proved in Theorems 4.22, 4.24, and 4.33, which indicate that a small positive* Q *can strengthens or reduce the current* I *based on (4.2).*

To illustrate some analytical results in Theorems 4.22, 4.24, and 4.33, numerical simulations on the I-V relation are carried out and shown in Figure 5.

From Figure 5, the following can be seen:

(I) $Q = 0$, that is, without the permanent charge, then the I-V relation is a straight line.

(II) $Q = 0.05$, and $\mu = 0$, that is, the permanent charge has one nonzero region, and a small positive Q can strengthens or reduce the current I.

(III) $Q = 0.05, \mu = 1$ or $Q = 0.05, \mu = -2$, that is, the permanent charges have two nonzero regions, and a small positive Q can furthermore strengthens or reduce the current I.

Also, the following can be easily verified:

Proposition 4.36. *The critical potentials* $V_{rev}(L,R)$, $V^0(L,R)$, $V_q^0(L,R)$, *and* $V_q^{\pm}(L,R)$ *scale invariantly in* (L,R).

Proof. From the expression for $V_{rev}(L,R)$ in (4.23), it can be seen that $V_{rev}(L,R)$ scales invariantly in (L,R). From Lemma 4.1, it follows that A_1, B_1, A_2, and B_2 scale invariantly in (L,R). Therefore, based on (4.22), it can be seen that the critical potentials $V^0(L,R)$, $V_q^0(L,R)$, and $V_q^{\pm}(L,R)$, as roots of $P(V;L,R) = 0$, scale invariantly in (L,R) accordingly.

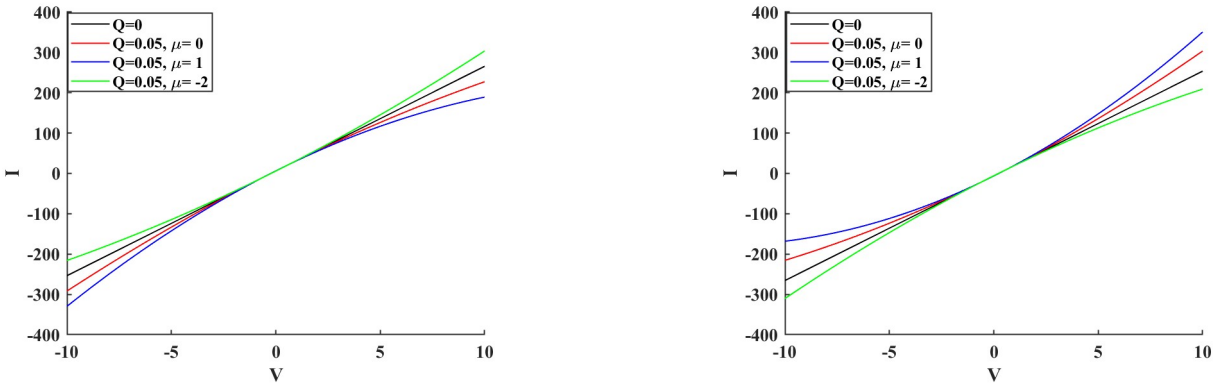

Figure 5. The parameters are chosen as $z_1 = 1, z_2 = -1, D_1 = 4, D_2 = 2, \alpha_1 = 0.2, \beta_1 = 0.4, \alpha_2 = 0.6, \beta_2 = 0.8$ and $H(1) = 1$. The left image and right image correspond to $L = 6, R = 3$ and $L = 3, R = 6$, respectively.

5. Conclusions

The PNP model is a very popular continuum theory describing ion transport in complex biological systems. With the electrochemical potential in (1.4) and the permanent charge in (1.8), the classical PNP model including two oppositely charged ions is used in this paper to study the effects of the small permanent charge and channel geometry $(\alpha_1, \beta_1, \alpha_2, \beta_2)$ on ionic flows. By employing the geometric singular perturbation theory and a regular perturbation expansion, we obtain explicit expressions for the first-order approximation J_{i1} in (3.3) of individual flux, which is a very complicated function of multiple variables. Based on the properties of J_{i1}, the effects of the permanent charge on the fluxes is analyzed in Theorems 4.7, 4.8, 4.12, and 4.13, which indicate that small $|Q|$ strengthens or reduces the individual flux. Under some conditions, the critical potentials and the signs of $\bar{I}_1$ are justified in Theorems 4.22, 4.24, and 4.33. Also, various conditions for the maximum of J_{i1} are identified in Proposition 4.17, which are related to the structures of the ion channels, namely, the ion channels have a short and narrow cross-section.

Relative to the article [1], there are some differences due to the permanent charge in (1.8). Specifically, the ratio $\mu = \dfrac{Q_2}{Q_1}$ is an additional parameter included in our analysis. Lemma 4.6 is also a new result related to the channel geometry $(\alpha_1, \beta_1, \alpha_2, \beta_2)$. Moreover J_{i1} is a function in multivariables $\alpha_1, \beta_1, \alpha_2, \beta_2$, and μ. On the other hand, it can be seen that as $Q_1 = 0$ or $Q_2 = 0$ in (1.8), the formula for J_{i1} in Proposition 3.4 is the same as that in [1], and the results in this paper can be reduced to those in [1].

The function J_{i1} in (3.3) explicitly depends on the boundary conditions, the channel geometry $(\alpha_1, \beta_1, \alpha_2, \beta_2)$, and μ in a very complicated way. Therefore, it is very convenient to carry out extensive numerical experiments on the individual flux.

In this paper, due to the one-dimensional version of the steady-state PNP model under study, there are some existing results, such as finite-dimensional geometric singular perturbation theory and the exchange

lemma, which can be employed to prove the existence of a unique solution for (2.8) in the vicinity of a singular orbit for small Q and small $\varepsilon > 0$. Afterwards, the effects of the small permanent charge and channel geometry on ionic flow can be further analyzed. However, it is very challenging as to whether a two-dimensional version or three-dimensional version of the steady-state PNP model can be theoretically analyzed in a similar way. From a dynamical view, a two-dimensional version or three-dimensional version of the steady-state PNP model is an infinite-dimensional dynamical system. Recently, in [61], finite-dimensional geometric singular perturbation theory is extended to an infinite-dimensional version, which can be used to analyze fast-slow systems of partial differential equations.

Apart from mathematical analysis of the dynamics of the one-dimensional version of the steady-state PNP model, there are extensive numerical works for the PNP system [62–67]. In particular, Liu et al. [64–66] proposed both the first-order and second-order numerical schemes which preserve three theoretical properties: unique solvability/positivity-preserving, unconditional energy stability, and optimal rate convergence analysis in the energetic variational formulation. Since the ion concentration must be non-negative, numerical algorithms preserving positivity proposed in [64–66] will be very important for the ion concentrations. Accordingly, it is an important problem whether numerical algorithms developed in [64–66] can be applicable to the PNP model studied in this article.

Use of AI tools declaration

The author declares he has not used Artificial Intelligence (AI) tools in the creation of this article.

Acknowledgments

The author thanks the referees very much for their careful reviews and comments that helped improve the manuscript. The author was supported by the NNSFC 12131007.

Conflict of interest

The author declares there is no conflict of interest.

References

1. S. Ji, W. Liu, M. Zhang, Effects of (small) permanent charge and channel geometry on ionic flows via classical Poisson–Nernst–Planck models, *SIAM J. Appl. Math.*, **75** (2015), 114–135. https://doi.org/10.1137/140992527
2. S. Chung, S. Kuyucak, Recent advances in ion channel research, *Biochim. Biophys. Acta*, **1565** (2002), 267–286. https://doi.org/10.1016/s0005-2736(02)00574-6
3. B. Corry, T. Allen, S. Kuyucak, S. Chung, Mechanisms of permeation and selectivity in calcium channels, *Biophys. J.*, **80** (2001), 195–214. https://doi.org/10.1016/S0006-3495(01)76007-9
4. H. Hwang, G. Schatz, M. Ratner, Incorporation of inhomogeneous ion diffusion coefficients into kinetic lattice grand canonical Monte Carlo simulations and application to ion current calculations in a simple model ion channel, *J. Phys. Chem. A*, **111** (2007), 12506–12512. https://doi.org/10.1021/jp075838o

5. B. Roux, T. Allen, S. Bernèche, W. Im, Theoretical and computational models of biological ion channels, *Q. Rev. Biophys.*, **37** (2004), 15–103. https://doi.org/10.1017/s0033583504003968

6. D. Tieleman, P. Biggin, G. Smith, M. Sansom, Simulation approaches to ion channel structure-function relationships, *Q. Rev. Biophys.*, **34** (2001), 473–561. https://doi.org/10.1017/s0033583501003729

7. D. P. Chen, R. S. Eisenberg, Charges, currents and potentials in ionic channels of one conformation, *Biophys. J.*, **64** (1993), 1405–1421. https://doi.org/10.1016/S0006-3495(93)81507-8

8. R. D. Coalson, Discrete-state model of coupled ion permeation and fast gating in ClC chloride channels, *J. Phys. A*, **41** (2009), 115001. https://doi.org/10.1088/1751-8113/41/11/115001

9. B. Eisenberg, Ion channels as devices, *J. Comput. Electron.*, **2** (2003), 245–249. https://doi.org/10.1023/B:JCEL.0000011432.03832.22

10. B. Eisenberg, Proteins, channels, and crowded ions, *Biophys. Chem.*, **100** (2003), 507–517. https://doi.org/10.1016/S0301-4622(02)00302-2

11. D. Gillespie, R. S. Eisenberg, Physical descriptions of experimental selectivity measurements in ion channels, *Eur. Biophys. J.*, **31** (2002), 454–466. https://doi.org/10.1007/s00249-002-0239-x

12. D. Gillespie, W. Nonner, R. S. Eisenberg, Coupling Poisson-Nernst-Planck and density functional theory to calculate ion flux, *J. Phys. Condens. Matter*, **14** (2002), 12129–12145. https://doi.org/10.1088/0953-8984/14/46/317

13. W. Im, D. Beglov, B. Roux, Continuum solvation model: Electrostatic forces from numerical solutions to the Poisson-Bolztmann equation, *Comput. Phys. Commun.*, **111** (1998), 59–75. https://doi.org/10.1016/S0010-4655(98)00016-2

14. S. Y. Noskov, S. Berneche, B. Roux, Control of ion selectivity in potassium channels by electrostatic and dynamic properties of carbonyl ligands, *Nature*, **431** (2004), 830–834. https://doi.org/10.1038/nature02943

15. S. Y. Noskov, B. Roux, Ion selectivity in potassium channels, *Biophys. Chem.*, **124** (2006), 279–291. https://doi.org/10.1016/j.bpc.2006.05.033

16. D. Boda, D. Busath, B. Eisenberg, D. Henderson, W. Nonner, Monte Carlo simulations of ion selectivity in a biological Na channel: Charge-space competition, *Phys. Chem. Chem. Phys.*, **4** (2002), 5154–5160. https://doi.org/10.1039/B203686J

17. S. Chung, S. Kuyucak, Predicting channel function from channel structure using Brownian dynamics simulations, *Clin. Exp. Pharmacol. Physiol.*, **28** (2001), 89–94. https://doi.org/10.1046/j.1440-1681.2001.03408.x

18. W. Im, B. Roux, Ion permeation and selectivity of OmpF porin: A theoretical study based on molecular dynamics, Brownian dynamics, and continuum electrodiffusion theory, *J. Mol. Biol.*, **322** (2002), 851–869. https://doi.org/10.1016/S0022-2836(02)00778-7

19. S. Y. Noskov, W. Im, B. Roux, Ion permeation through the α-hemolysin channel: Theoretical studies based on brownian dynamics and Poisson-Nernst-Planck electrodiffusion theory, *Biophys. J.*, **87** (2004), 2299–2309. https://doi.org/10.1529/biophysj.104.044008

20. Z. Schuss, B. Nadler, R. S. Eisenberg, Derivation of Poisson and Nernst-Planck equations in a bath and channel from a molecular model, *Phys. Rev. E*, **64** (2001), 1–14. https://doi.org/10.1103/PhysRevE.64.036116
21. V. Barcilon, Ion flow through narrow membrane channels: Part I, *SIAM J. Appl. Math.*, **52** (1992), 1391–1404. https://doi.org/10.1137/0152080
22. B. Eisenberg, Y. Hyon, C. Liu, Energy variational analysis of ions in water and channels: Field theory for primitive models of complex ionic fluids, *J. Chem. Phys.*, **133** (2010), 104104. https://doi.org/10.1063/1.3476262
23. B. Eisenberg, Y. Hyon, C. Liu, Energy variational analysis *EnVarA* of ions in calcium and sodium channels, *Biophys. J.*, **98** (2010), 515A. https://doi.org/10.1016/j.bpj.2009.12.2802
24. Y. Hyon, B. Eisenberg, C. Liu, A mathematical model for the hard sphere repulsion in ionic solutions, *Commun. Math. Sci.*, **9** (2010), 459–475. https://doi.org/10.4310/cms.2011.v9.n2.a5
25. Y. Hyon, J. Fonseca, B. Eisenberg, C. Liu, A new Poisson-Nernst-Planck equation (PNP-FS-IF) for charge inversion near walls, *Biophys. J.*, **100** (2011), 578A. https://doi.org/10.1016/j.bpj.2010.12.3342
26. P. M. Biesheuvel, Two-fluid model for the simultaneous flow of colloids and fluids in porous media, *J. Colloid Interface Sci.*, **355** (2011), 389–395. https://doi.org/10.1016/j.jcis.2010.12.006
27. D. Chen, R. Eisenberg, J. Jerome, C. Shu, Hydrodynamic model of temperature change in open ionic channels, *Biophys. J.*, **69** (1995), 2304–2322. https://doi.org/10.1016/S0006-3495(95)80101-3
28. J. Jerome, *Analysis of Charge Transport: A Mathematical Study of Semiconductor Devices*, Springer-Verlag, New York, 1995. https://doi.org/10.1007/978-3-642-79987-7
29. Y. Wang, K. Pant, Z. Chen, G. Wang, W. Diffey, P. Ashley, et al., Numerical analysis of electrokinetic transport in micro-nanofluidic interconnect preconcentrator in hydrodynamic flow, *Microfluid. Nanofluid.*, **7** (2009), 683–696. https://doi.org/10.1007/s10404-009-0428-3
30. W. Liu, B. Wang, Poisson-Nernst-Planck systems for narrow tubular-like membrane channels, *J. Dyn. Differ. Equations*, **22** (2010), 413–437. https://doi.org/10.1007/s10884-010-9186-x DOI 10.1007/s10884-010-9186-x
31. W. Nonner, R. S. Eisenberg, Ion permeation and glutamate residues linked by Poisson-Nernst-Planck theory in L-type Calcium channels, *Biophys. J.*, **75** (1998), 1287–1305. https://doi.org/10.1016/S0006-3495(98)74048-2
32. M. Burger, R. S. Eisenberg, H. W. Engl, Inverse problems related to ion channel selectivity, *SIAM J. Appl. Math.*, **67** (2007), 960–989. https://doi.org/10.1137/060664689
33. A. E. Cardenas, R. D. Coalson, M. G. Kurnikova, Three-dimensional Poisson-Nernst-Planck theory studies: Influence of membrane electrostatics on gramicidin a channel conductance, *Biophys. J.*, **79** (2000), 80–93. https://doi.org/10.1016/S0006-3495(00)76275-8
34. M. Saraniti, S. Aboud, R. Eisenberg, The simulation of ionic charge transport in biological ion channels: An introduction to numerical methods, *Rev. Comput. Chem.*, **22** (2005), 229–294. https://doi.org/10.1002/0471780367.ch4
35. V. Barcilon, D. P. Chen, R. S. Eisenberg, Ion flow through narrow membrane channels: Part II, *SIAM J. Appl. Math.*, **52** (1992), 1405–1425. https://doi.org/10.1137/0152081

36. P. Bates, Y. Jia, G. Lin, H. Lu, M. Zhang, Individual flux study via steady-state Poisson-Nernst-Planck systems: Effects from boundary conditions, *SIAM J. Appl. Dyn. Syst.*, **16** (2017), 410–430. https://doi.org/10.1137/16M1071523

37. B. Eisenberg, W. Liu, Poisson-Nernst-Planck systems for ion channels with permanent charges, *SIAM J. Math. Anal.*, **38** (2007), 1932–1966. https://doi.org/10.1137/060657480

38. A. Singer, D. Gillespie, J. Norbury, R. S. Eisenberg, Singular perturbation analysis of the steady-state Poisson-Nernst-Planck system: Applications to ion channels, *Eur. J. Appl. Math.*, **19** (2008), 541–569. https://doi.org/10.1017/S0956792508007596

39. W. Liu, Geometric singular perturbation approach to steady-state Poisson-Nernst-Planck systems, *SIAM J. Appl. Math.*, **65** (2005), 754–766. https://doi.org/10.1137/S0036139903420931

40. W. Liu, One-dimensional steady-state Poisson-Nernst-Planck systems for ion channels with multiple ion species, *J. Differ. Equations*, **246** (2009), 428–451. https://doi.org/10.1016/j.jde.2008.09.010

41. W. Liu, H. Xu, A complete analysis of a classical Poisson-Nernst-Planck model for ionic flow, *J. Differ. Equations*, **258** (2015), 1192–1228. https://doi.org/10.1016/j.jde.2014.10.015

42. H. Mofidi, B. Eisenberg, W. Liu, Effects of diffusion coefficients and permanent charge on reversal potentials in ionic channels, *Entropy*, **22** (2020), 1–23. https://doi.org/10.3390/e22030325

43. H. Mofidi, W. Liu, Reversal potential and reversal permanent charge with unequal diffusion coefficients via classical Poisson–Nernst–Planck models, *SIAM J. Appl. Math.*, **80** (2020), 1908–1935. https://doi.org/10.1137/19M1269105

44. H. Mofidi, New insights into the effects of small permanent charge on ionic flows: A higher order analysis, *Math. Biosci. Eng.*, **21** (2024), 6042–6076. https://doi.org/10.3934/mbe.2024266

45. J. K. Park, J. W. Jerome, Qualitative properties of steady-state Poisson-Nernst-Planck systems: Mathematical study, *SIAM J. Appl. Math.*, **57** (1997), 609–630. https://doi.org/10.1137/S0036139995279809

46. I. Rubinstein, Multiple steady states in one-dimensional electrodiffusion with local electroneutrality, *SIAM J. Appl. Math.*, **47** (1987), 1076–1093. https://doi.org/10.1137/0147070

47. A. Singer, J. Norbury, A Poisson-Nernst-Planck model for biological ion channels—An asymptotic analysis in a three-dimensional narrow funnel, *SIAM J. Appl. Math.*, **70** (2009), 949–968. https://doi.org/10.1137/070687037

48. A. Singer, D. Gillespie, J. Norbury, R. S. Eisenberg, Singular perturbation analysis of the steady-state Poisson-Nernst-Planck system: Applications to ion channels, *Eur. J. Appl. Math.*, **19** (2008), 541–560. https://doi.org/10.1017/S0956792508007596

49. H. Steinrück, A bifurcation analysis of the one-dimensional steady-state semiconductor device equations, *SIAM J. Appl. Math.*, **49** (1989), 1102–1121. https://doi.org/10.1137/0149066

50. L. Zhang, W. Liu, Effects of large permanent charges on ionic flows via Poisson-Nernst-Planck models, *SIAM J. Appl. Dyn. Syst.*, **19** (2020), 1993–2029. https://doi.org/10.1137/19M1289443

51. B. Corry, S. Kuyucak, S. H. Chung, Dielectric self-energy in Poisson-Boltzmann and Poisson Nernst-Planck models of ion channels, *Biophys. J.*, **84** (2003), 3594–3606. https://doi.org/10.1016/S0006-3495(03)75091-7

52. M. S. Kilic, M. Z. Bazant, A. Ajdari, Steric effects in the dynamics of electrolytes at large applied voltages. II. Modified Poisson-Nernst-Planck equations, *Phys. Rev. E*, **75** (2007), 021503. https://doi.org/10.1103/PhysRevE.75.021503

53. A. Mamonov, R. Coalson, A. Nitzan, M. Kurnikova, The role of the dielectric barrier in narrow biological channels: A novel composite approach to modeling single-channel currents, *Biophys. J.*, **84** (2003), 3646–3661. https://doi.org/10.1016/S0006-3495(03)75095-4

54. D. Gillespie, W. Nonner, R. S. Eisenberg, Crowded charge in biological ion channels, *Nanotech*, **3** (2003), 435–438. https://doi.org/10.1002/9781118158715.ch2

55. S. Ji, W. Liu, Poisson-Nernst-Planck systems for ion flow with density functional theory for hard-sphere potential: I-V relations and critical potentials. Part I: Analysis, *J. Dyn. Differ. Equations*, **24** (2012), 955–983. https://doi.org/10.1007/s10884-012-9277-y

56. G. Lin, W. Liu, Y. Yi, M. Zhang, Poisson-Nernst-Planck systems for ion flow with density functional theory for local hard-sphere potential, *SIAM J. Appl. Dyn. Syst.*, **12** (2013), 1613–1648. https://doi.org/10.1137/120904056

57. G. Lin, Effects of ion sizes on Poisson–Nernst–Planck systems with multiple ions, *Math. Meth. Appl. Sci.*, **46** (2022), 1–27. https://doi.org/10.1002/mma.8954

58. W. Huang, W. Liu, Y. Yu, Permanent charge effects on ionic flow: A numerical study of flux ratios and their bifurcation, *Commun. Comput. Phys.*, **30** (2021), 486–514. https://doi.org/10.4208/cicp.OA-2020-0057

59. C. Jones, Geometric singular perturbation theory, in *Dynamical Systems. Lecture Notes in Mathematics*, Springer-Verlag, Berlin, **1609** (1995), 44–118. https://doi.org/10.1007/BFB0095239

60. C. Jones, N. Kopell, Tracking invariant manifolds with differential forms in singularly perturbed systems, *J. Differ. Equations*, **108** (1994), 64–88. https://doi.org/10.1006/jdeq.1994.1025

61. F. Hummel, C. Kuehn, Slow manifolds for infinite-dimensional evolution equations, *Comment. Math. Helv.*, **97** (2022), 61–132. https://doi.org/10.4171/CMH/527

62. L. Dong, D. He, Y. Qin, Z. Zhang, A positivity-preserving, linear, energy stable and convergent numerical scheme for the Poisson–Nernst–Planck (PNP) system, *J. Comput. Appl. Math.*, **444** (2023), 115784. https://doi.org/10.1016/j.cam.2024.115784

63. D. He, K. Pan, X. Yue, A positivity preserving and free energy dissipative difference scheme for the Poisson–Nernst–Planck system, *J. Sci. Comput.*, **81** (2019), 436–458. https://doi.org/10.1007/s10915-019-01025-x

64. C. Liu, C. Wang, S. M. Wise, X. Yue, S. Zhou, A positivity preserving energy stable and convergent numerical scheme for the Poisson-Nernst-Planck system, *Math. Comput.*, **90** (2021), 2071–2106. https://doi.org/10.1090/mcom/3642

65. C. Liu, C. Wang, S. M. Wise, X. Yue, S. Zhou, An iteration solver for the Poisson-Nernst-Planck system and its convergence analysis, *J. Comput. Appl. Math.*, **406** (2022), 114017. https://doi.org/10.1016/j.cam.2021.114017

66. C. Liu, C. Wang, S. M. Wise, X. Yue, S. Zhou, A second order accurate, positivity preserving numerical method for the Poisson–Nernst–Planck system and its convergence analysis, *J. Sci. Comput.*, **97** (2023), 23. https://doi.org/10.1007/s10915-023-02345-9

67. J. Shen, X. Jie, Unconditionally positivity preserving and energy dissipative schemes for Poisson–Nernst– Planck equations, *Numer. Math.*, **148** (2021), 671–697. https://doi.org/10.1007/s00211-021-01203-w

Appendix

In this section, we give a proof of Proposition 3.4.

Proof. First, by substituting (3.1) into (2.8) and Table 1, the following formulae can be obtained.

Lemma 5.1. *One has*

$$z_1c_{11}^{a_1}+z_2c_{21}^{a_1}=-\frac{1}{2},\ \phi_1^{a_1,r}=\phi_1^{a_1}+\frac{1}{2z_1(z_1-z_2)c_{10}^{a_1}},$$

$$z_1c_{11}^{b_1}+z_2c_{21}^{b_1}=-\frac{1}{2},\ \phi_1^{b_1,l}=\phi_1^{b_1}+\frac{1}{2z_1(z_1-z_2)c_{10}^{b_1}},$$

$$z_1c_{11}^{a_2}+z_2c_{21}^{a_2}=-\frac{\mu}{2},\ \phi_1^{a_2,r}=\phi_1^{a_2}+\frac{\mu}{2z_1(z_1-z_2)c_{10}^{a_2}},$$

$$z_1c_{11}^{b_2}+z_2c_{21}^{b_2}=-\frac{\mu}{2},\ \phi_1^{b_2,l}=\phi_1^{b_2}+\frac{\mu}{2z_1(z_1-z_2)c_{10}^{b_2}},$$

$$\phi_1^{a_1,l}=\phi_1^{a_1}-\frac{c_{10}^{a_1}c_{21}^{a_1}-c_{20}^{a_1}c_{11}^{a_1}}{(z_1-z_2)c_{10}^{a_1}c_{20}^{a_1}},\ c_{11}^{a_1,l}=\frac{z_2(c_{11}^{a_1}+c_{21}^{a_1})}{z_2-z_1},\ c_{21}^{a_1,l}=\frac{z_1(c_{11}^{a_1}+c_{21}^{a_1})}{z_1-z_2},$$

$$c_{11}^{a_1,r}=c_{11}^{a_1}-\frac{1}{2(z_1-z_2)},\ c_{11}^{b_1,l}=c_{11}^{b_1}-\frac{1}{2(z_1-z_2)},$$

$$\phi_1^{b_1,r}=\phi_1^{b_1}-\frac{c_{10}^{b_1}c_{21}^{b_1}-c_{20}^{b_1}c_{11}^{b_1}}{(z_1-z_2)c_{10}^{b_1}c_{20}^{b_1}},\ c_{11}^{b_1,r}=\frac{z_2(c_{11}^{b_1}+c_{21}^{b_1})}{z_2-z_1},\ c_{21}^{b_1,r}=\frac{z_1(c_{11}^{b_1}+c_{21}^{b_1})}{z_1-z_2},$$

$$\phi_1^{a_2,l}=\phi_1^{a_2}-\frac{c_{10}^{a_2}c_{21}^{a_2}-c_{20}^{a_2}c_{11}^{a_2}}{(z_1-z_2)c_{10}^{a_2}c_{20}^{a_2}},\ c_{11}^{a_2,l}=\frac{z_2(c_{11}^{a_2}+c_{21}^{a_2})}{z_2-z_1},\ c_{21}^{a_2,l}=\frac{z_1(c_{11}^{a_2}+c_{21}^{a_2})}{z_1-z_2},$$

$$c_{11}^{a_2,r}=c_{11}^{a_2}-\frac{\mu}{2(z_1-z_2)},\ c_{11}^{b_2,l}=c_{11}^{b_2}-\frac{\mu}{2(z_1-z_2)},$$

$$\phi_1^{b_2,r}=\phi_1^{b_2}-\frac{c_{10}^{b_2}c_{21}^{b_2}-c_{20}^{b_2}c_{11}^{b_2}}{(z_1-z_2)c_{10}^{b_2}c_{20}^{b_2}},\ c_{11}^{b_2,r}=\frac{z_2(c_{11}^{b_2}+c_{21}^{b_2})}{z_2-z_1},\ c_{21}^{b_2,r}=\frac{z_1(c_{11}^{b_2}+c_{21}^{b_2})}{z_1-z_2}.$$

Then, by using the results in Proposition 3.2 and Lemma 5.1, and by substituting (3.1) into (2.8) and Table 1, one obtains

$$
\begin{aligned}
J_{11} = &-\frac{z_1(c_{10}^{b_1}-c_{10}^{a_2})}{(\alpha_2-\beta_1)H(1)(\ln c_{10}^{b_1}-\ln c_{10}^{a_2})}\Big[\phi_1^{a_2}-\frac{c_{10}^{a_2}c_{21}^{a_2}-c_{20}^{a_2}c_{11}^{a_2}}{(z_1-z_2)c_{10}^{a_2}c_{20}^{a_2}}\\
&-\frac{z_2(c_{11}^{a_2}+c_{21}^{a_2})}{z_2-z_1}\frac{\phi_0^{b_1}-\phi_0^{a_2}}{c_{10}^{a_2}(\ln c_{10}^{b_1}-\ln c_{10}^{a_2})}-\phi_1^{b_1}+\frac{c_{10}^{b_1}c_{21}^{b_1}-c_{20}^{b_1}c_{11}^{b_1}}{(z_1-z_2)c_{10}^{b_1}c_{20}^{b_1}}\\
&+\frac{z_2(c_{11}^{b_1}+c_{21}^{b_1})}{z_2-z_1}\frac{\phi_0^{b_1}-\phi_0^{a_2}}{c_{10}^{b_1}(\ln c_{10}^{b_1}-\ln c_{10}^{a_2})}\Big]\\
&+\frac{z_2(c_{11}^{b_1}+c_{21}^{b_1})}{(z_2-z_1)(\alpha_2-\beta_1)H(1)}\Big[1+\frac{z_1(\phi_0^{b_1}-\phi_0^{a_2})}{\ln c_{10}^{b_1}-\ln c_{10}^{a_2}}\Big]\\
&-\frac{z_2(c_{11}^{a_2}+c_{21}^{a_2})}{(z_2-z_1)(\alpha_2-\beta_1)H(1)}\Big[1+\frac{z_1(\phi_0^{b_1}-\phi_0^{a_2})}{\ln c_{10}^{b_1}-\ln c_{10}^{a_2}}\Big]\\
= &-\frac{z_1(c_1^{L}-c_{10}^{a_1})}{\alpha_1 H(1)(\ln c_1^{L}-\ln c_{10}^{a_1})}\Big[\phi_1^{a_1}-\frac{c_{10}^{a_1}c_{21}^{a_1}-c_{20}^{a_1}c_{11}^{a_1}}{(z_1-z_2)c_{10}^{a_1}c_{20}^{a_1}}\\
&-\frac{z_2(c_{11}^{a_1}+c_{21}^{a_1})}{z_2-z_1}\frac{\phi^{L}-\phi_0^{a_1}}{c_{10}^{a_1}(\ln c_1^{L}-\ln c_{10}^{a_1})}\Big]\\
&-\frac{z_2(c_{11}^{a_1}+c_{21}^{a_1})}{(z_2-z_1)\alpha_1 H(1)}\Big[1+\frac{z_1(\phi^{L}-\phi_0^{a_1})}{\ln c_1^{L}-\ln c_{10}^{a_1}}\Big]\\
= &\frac{z_1(c_{10}^{b_2}-c_1^{R})}{(1-\beta_2)H(1)(\ln c_{10}^{b_2}-\ln c_1^{R})}\Big[\phi_1^{b_2}-\frac{c_{10}^{b_2}c_{21}^{b_2}-c_{20}^{b_2}c_{11}^{b_2}}{(z_1-z_2)c_{10}^{b_2}c_{20}^{b_2}}\\
&-\frac{z_2(c_{11}^{b_2}+c_{21}^{b_2})}{z_2-z_1}\frac{\phi_0^{b_2}-\phi^{R}}{c_{10}^{b_2}(\ln c_{10}^{b_2}-\ln c_1^{R})}\Big]\\
&+\frac{z_2(c_{11}^{b_2}+c_{21}^{b_2})}{(z_2-z_1)(1-\beta_2)H(1)}\Big[1+\frac{z_1(\phi_0^{b_2}-\phi^{R})}{\ln c_{10}^{b_2}-\ln c_1^{R}}\Big],
\end{aligned}
\tag{5.1}
$$

$$
\begin{aligned}
J_{21} = &-\frac{z_2(c_{20}^{b_1}-c_{20}^{a_2})}{(\alpha_2-\beta_1)H(1)(\ln c_{20}^{b_1}-\ln c_{20}^{a_2})}\Big[\phi_1^{a_2}-\frac{c_{10}^{a_2}c_{21}^{a_2}-c_{20}^{a_2}c_{11}^{a_2}}{(z_1-z_2)c_{10}^{a_2}c_{20}^{a_2}}\\
&-\frac{z_1(c_{11}^{a_2}+c_{21}^{a_2})}{z_1-z_2}\frac{\phi_0^{b_1}-\phi_0^{a_2}}{c_{20}^{a_2}(\ln c_{20}^{b_1}-\ln c_{20}^{a_2})}-\phi_1^{b_1}+\frac{c_{10}^{b_1}c_{21}^{b_1}-c_{20}^{b_1}c_{11}^{b_1}}{(z_1-z_2)c_{10}^{b_1}c_{20}^{b_1}}\\
&+\frac{z_1(c_{11}^{b_1}+c_{21}^{b_1})}{z_1-z_2}\frac{\phi_0^{b_1}-\phi_0^{a_2}}{c_{20}^{b_1}(\ln c_{20}^{b_1}-\ln c_{20}^{a_2})}\Big]\\
&+\frac{z_1(c_{11}^{b_1}+c_{21}^{b_1})}{(z_1-z_2)(\alpha_2-\beta_1)H(1)}\Big[1+\frac{z_2(\phi_0^{b_1}-\phi_0^{a_2})}{\ln c_{20}^{b_1}-\ln c_{20}^{a_2}}\Big]\\
&-\frac{z_1(c_{11}^{a_2}+c_{21}^{a_2})}{(z_1-z_2)(\alpha_2-\beta_1)H(1)}\Big[1+\frac{z_2(\phi_0^{b_1}-\phi_0^{a_2})}{\ln c_{20}^{b_1}-\ln c_{20}^{a_2}}\Big]\\
=&-\frac{z_2(c_2^{L}-c_{20}^{a_1})}{\alpha_1 H(1)(\ln c_2^{L}-\ln c_{20}^{a_1})}\Big[\phi_1^{a_1}-\frac{c_{10}^{a_1}c_{21}^{a_1}-c_{20}^{a_1}c_{11}^{a_1}}{(z_1-z_2)c_{10}^{a_1}c_{20}^{a_1}}\\
&-\frac{z_1(c_{11}^{a_1}+c_{21}^{a_1})}{z_1-z_2}\frac{\phi^{L}-\phi_0^{a_1}}{c_{20}^{a_1}(\ln c_2^{L}-\ln c_{20}^{a_1})}\Big]\\
&-\frac{z_1(c_{11}^{a_1}+c_{21}^{a_1})}{(z_1-z_2)\alpha_1 H(1)}\Big[1+\frac{z_2(\phi^{L}-\phi_0^{a_1})}{\ln c_2^{L}-\ln c_{20}^{a_1}}\Big]\\
=&\frac{z_2(c_{20}^{b_2}-c_2^{R})}{(1-\beta_2)H(1)(\ln c_{20}^{b_2}-\ln c_2^{R})}\Big[\phi_1^{b_2}-\frac{c_{10}^{b_2}c_{21}^{b_2}-c_{20}^{b_2}c_{11}^{b_2}}{(z_1-z_2)c_{10}^{b_2}c_{20}^{b_2}}\\
&-\frac{z_1(c_{11}^{b_2}+c_{21}^{b_2})}{z_1-z_2}\frac{\phi_0^{b_2}-\phi^{R}}{c_{20}^{b_2}(\ln c_{20}^{b_2}-\ln c_2^{R})}\Big]\\
&+\frac{z_1(c_{11}^{b_2}+c_{21}^{b_2})}{(z_1-z_2)(1-\beta_2)H(1)}\Big[1+\frac{z_2(\phi_0^{b_2}-\phi^{R})}{\ln c_{20}^{b_2}-\ln c_2^{R}}\Big],
\end{aligned}
\tag{5.2}
$$

and

$$
\begin{aligned}
&\phi_1^{b_1} = \phi_1^{a_1} + \frac{c_{10}^{b_1} - c_{10}^{a_1}}{2z_1(z_1 - z_2)c_{10}^{a_1}c_{10}^{b_1}} - (z_1J_{10} + z_2J_{20})y_{11} - (z_1J_{11} + z_2J_{21})y_{10},\\
&c_{11}^{b_1} = \left[c_{11}^{a_1} - \frac{1}{2(z_1 - z_2)} + \frac{J_{10}}{z_1(J_{10} + J_{20})}\right]\frac{c_{10}^{b_1}}{c_{10}^{a_1}} + \frac{1}{2(z_1 - z_2)}\\
&\quad + z_1z_2[(J_{10} + J_{20})y_{11} + (J_{11} + J_{21})y_{10}]c_{10}^{b_1} - \frac{J_{10}}{z_1(J_{10} + J_{20})},\\
&J_{11} + J_{21} = \frac{(z_2 - z_1)(c_{11}^{a_1} - c_{11}^{b_1})}{z_2(\beta_1 - \alpha_1)H(1)} - \frac{\phi_0^{a_1} - \phi_0^{b_1}}{(\beta_1 - \alpha_1)H(1)},\\
&\phi_1^{b_2} = \phi_1^{a_2} + \frac{(c_{10}^{b_2} - c_{10}^{a_2})\mu}{2z_1(z_1 - z_2)c_{10}^{a_2}c_{10}^{b_2}} - (z_1J_{10} + z_2J_{20})y_{21} - (z_1J_{11} + z_2J_{21})y_{20},\\
&c_{11}^{b_2} = \left[c_{11}^{a_2} - \frac{\mu}{2(z_1 - z_2)} + \frac{J_{10}\cdot\mu}{z_1(J_{10} + J_{20})}\right]\frac{c_{10}^{b_2}}{c_{10}^{a_2}} + \frac{\mu}{2(z_1 - z_2)}\\
&\quad + z_1z_2[(J_{10} + J_{20})y_{21} + (J_{11} + J_{21})y_{20}]c_{10}^{b_2} - \frac{J_{10}\cdot\mu}{z_1(J_{10} + J_{20})},\\
&J_{11} + J_{21} = \frac{(z_2 - z_1)(c_{11}^{a_2} - c_{11}^{b_2})}{z_2(\beta_2 - \alpha_2)H(1)} - \frac{(\phi_0^{a_2} - \phi_0^{b_2})\mu}{(\beta_2 - \alpha_2)H(1)}.
\end{aligned}
\tag{5.3}
$$

Finally, by solving the linear algebraic equations in (5.1)–(5.3), Proposition 3.4 is proved.